SIMULCASTING USING SLOTTED ALOHA IN AD-HOC NETWORKS

By

KIUNG JUNG

A DISSERTATION PRESENTED TO THE GRADUATE SCHOOL
OF THE UNIVERSITY OF FLORIDA IN PARTIAL FULFILLMENT
OF THE REQUIREMENTS FOR THE DEGREE OF
DOCTOR OF PHILOSOPHY

UNIVERSITY OF FLORIDA

2006

To my parents ...

LIST OF TABLES

LIST OF FIGURES

Abstract of Dissertation Presented to the Graduate School
of the University of Florida in Partial Fulfillment of the
Requirements for the Degree of Doctor of Philosophy

SIMULCASTING USING SLOTTED ALOHA IN AD-HOC NETWORKS

By

Kiung Jung

August 2006

Chair: John M. Shea
Major Department: Electrical and Computer Engineering

Previous studies used unequal error-protection techniques to improve the throughput of a wireless communication system in which a transmission is received by several radios with different capabilities. These capabilities may correspond to differences in path loss, fading, or interference. By taking advantage of the broadcast nature of the channel, additional messages for the more-capable receivers can be included on transmissions to the less-capable receivers at little cost (in terms of required energy at the transmitter or error probabilities at the receivers). This technique has been termed simulcasting or multicast signaling.

We consider this technique in an ad hoc network. This technique impacts link throughput, end-to-end throughput, and network connectivity. First, we investigated the basic properties of simulcasting, including how the choice of parameters for the simulcasting technique affects several key network performance metrics. The results show that a properly chosen simulcasting technique can improve the link and end-to-end throughput in ad hoc wireless networks with only a slight degradation in other metrics such as connectivity. Next, we propose cross-layer techniques for unequal resource allocation to improve network performance when using simulcasting. We then propose to

allocate the channel more often to radios that can simulcast. This unequal channel access is achieved by a simple modification to the back-off parameter in the MAC algorithm. We then consider the distribution of traffic over multiple routes according to the simulcasting capabilities of the radios along the routes. Finally, we propose schemes to adapt the transmit power and signal constellation shape based on the channel conditions to the intended receivers. Results show that these cross-layer approaches effectively enhance the performance of simulcasting in wireless ad hoc networks.

CHAPTER 1
INTRODUCTION

In most ad hoc wireless networks, a radio's neighbors often vary considerably in their ability to communicate with that radio because of differences in channel conditions, such as propagation loss and interference levels. In unicast transmissions, in which a single transmitter communicates with a single receiver, the transmitter can compensate for these variations in capability by using adaptive signaling if the channel conditions are accurately known. However, the shared channel is not necessarily used effectively because a signal that is intended for one radio may also be received by other radios in the system that have much better link conditions than the original destination receiver. We refer to such radios as more-capable radios. In this scenario, additional messages could be included for the more-capable radios at little expense to the original destination of the unicast transmission. Similarly, broadcast transmissions, which are intended for all of a radio's neighbors, are often required for network maintenance in ad hoc networks. Broadcast transmissions are generally ineffective in their use of the shared communication medium because the transmissions must be designed to allow reception by the least-capable of a radio's neighbors. Thus, for any broadcast transmission there are often many more-capable receivers that could successfully receive additional messages that are simultaneously transmitted with the broadcast message.

The concepts behind simultaneous transmissions schemes were originally explored in the context of broadcast channels by Cover and Bergmans [1], [2]. Pursley and Shea previously showed that modulation and coding schemes can be modified to allow the inclusion of additional messages for more-capable receivers at very little cost to the performance at the less-capable receiver [3]–[6]. In these papers, the term multicast signaling is used to refer to such techniques. However, in ad hoc networks, multicasting

refers to a process that is primarily associated with the network layer in which a single message is delivered to multiple destinations, not all of which are necessarily neighbors of the source radio. In this dissertation, we refer to our techniques as simulcasting to distinguish them from multicasting and to convey their ability to simultaneously transmit multiple messages to different neighboring radios of a transmitter. Previous work shows that nonuniform phase-shift-key (PSK) constellations provide a simple and effective way to convey multiple messages from a single transmitter to two receivers of different capabilities [3]–[6].

Unlike the previous work, which investigated the physical-layer design and performance of simulcasting schemes, we propose to investigate the opportunistic use of simulcasting in wireless ad hoc networks. We consider the necessary modifications to the higher-layer protocols to fully utilize the additional capabilities provided by simulcasting. For complete cross-layer design of such a wireless communication system with simulcasting, the link- and network- layer protocols including the packet selection algorithm, routing protocol, and collision resolution algorithm should be appropriately designed. The design of the simulcasting scheme will impact many aspects of network performance including link and end-to-end throughput, network connectivity, and route length. We investigate the optimal signal spacing for nonuniform quadrature phase-shift-keying (QPSK) for randomly distributed radios.

We consider a system that uses slotted ALOHA [7]–[11] for channel access. The routing algorithm used is a minimum-hop routing algorithm that is modified to incorporate the simulcasting capability. The packet selection mechanism is also modified to provide efficient use of the simulcasting capability. We use nonuniform PSK to show how the design of the simulcasting technique affects link throughput, end-to-end throughput, and network connectivity. We first present analytical and simulation results for random topologies with our simple “good/bad” channel model and with mobility. For the simple “good/bad” channel model, in which we do not consider any

interference, whether two radios are neighbors depends only on if one of the radios is in the transmission range of the other. In the “good/bad” channel model, the collision occurs when linked radio(s) to a receiver transmit(s) a packet simultaneously when the receiver receives another packet. The results indicate that simulcast transmission can improve the link and end-to-end throughputs in wireless ad hoc at a small cost to network connectivity.

We investigate three cross-layer approaches to improve network performance when simulcasting is used. First, we propose to adapt the parameters of the MAC protocol based on simulcasting capabilities. A radio that can simulcast to its neighbors can transmit two packets per slot, whereas a radio that cannot simulcast can only transmit one packet per slot. In the terminology of [12], the simulcasting radio requires less *effort* to transmit a packet than the unicasting radio. Thus, to improve link throughput, more channel resources should be allocated to simulcasting radios. We use Dianati et al.’s notion of *fair share* to determine the back-off parameters at different nodes to provide a balance between channel allocation that ignores effort and service based allocation [13]. These unequal back-off parameters can improve link throughput at the expense of fairness in the view point of eveness. For instance, the parameters can be such that a few radios will nearly always be able to transmit while the other radios are blocked. The link throughput increases because there are few collisions, but the network becomes useless as the end-to-end throughput decreases and most radios are unable to transmit any packets. Therefore, in comparing different back-off parameters, we also consider both the fairness provided and end-to-end throughput. We present fairness results using the typical min-max fairness index [14] and the utility-based fairness index introduced in [13].

Second, we consider how to take advantage of the simulcasting capability on a route to reduce queueing delay and improve end-to-end throughput. Because radios that can simulcast packets send more packets per transmission opportunity, it maybe appropriate to route more packets along routes with more more-capable links and with a greater

number of radios with more-capable links. We propose a simple scheme in which packets are distributed unequally across two routes according to a Bernoulli random process. We evaluate the effect of different choices for the Bernoulli parameter on the end-to-end throughput and delay for several network topologies. The results show that unequal distribution of the packets over the two routes offers the best performance in terms of end-to-end throughput and delay.

Third, we investigate adapting the transmission power and offset angle of the simulcasting modulation based on the number of neighbors of the transmitter. For systems in which the transmitted power is fixed, the transmission power under a certain radio density decides the network degree, which is defined as the average number of neighbors of a radio in a network, where two radios are neighbors if they can communicate directly. When the radios in a network use a large transmission range, the required number of hops for a transmitted packet to reach a destination from a source radio will be small. However, a large transmission range also results in a large network degree. From the perspective of a receiver, as interference from neighboring radios becomes large, the probability of packet collision will increase. The link throughput can be improved by decreasing the transmission power and hence the network degree. However, for low network degree, the probability that the network is connected will be small and the number of hops in a route will be large. So, the tradeoff among the effect of transmission range on probability of packet collision, number of hops in a route, and network connectivity is a critical problem to solve in an ad-hoc network.

We investigate schemes to adapt the transmission power and signal constellation shape based on the distances between the transmitter and the receiver(s). We consider unequal power allocation so that radios that can simulcast have a higher probability of packet success than radios that cannot simulcast. We present analytical and simulation results. The results indicate that the reduced transmission energy and the unequal

interference assignment schemes improve link and end-to-end throughput as well as throughput efficiency, which is defined as throughput per unit energy consumption.

As prior works of simulcasting, Cover [1] considers the simultaneous communication of information from one source to several receivers and gives upper and lower bounds on the capacity region of simultaneously achievable rates. Bergmans [2] considers several transmitters using a superposition scheme that pools the time, bandwidth, and power allocation of the transmitters. He determines the optimal set of rates simultaneously achievable.

Pursely and Shea have previously shown that modulation and coding schemes can be modified to allow the inclusion of additional messages for more-capable receivers at very little cost to the performance at the less-capable receiver [3]–[6]. This general technique is called multicast signaling and uses unequal error-protection signaling to transmit multiple messages that require different receiver capabilities for accurate reception. As previously mentioned, we use the term *simulcasting* for these techniques to distinguish them from network- or application- layer multicasting. In [3]-[6], the authors focus on techniques that utilize nonuniform phase-shift keying (PSK) because of its simplicity, adjustability, and constant envelope. This previous works is focused on physical-layer considerations, primarily signal design and link-level performance, although simulcast transmission also requires interactions with the higher layers in the protocol stack. They also introduce and analyze performance measures that are useful in characterizing the performance tradeoffs in simulcast packet transmission.

Simulcast transmission can be achieved through a variety of other unequal error-protection techniques. These include other types of nonuniform modulation [15]-[18], unequal error-protection coding [19]-[24], combined modulation and coding schemes [25]-[28], [5], and space-time coding [29]. Any of these techniques can be used for simulcasting in ad hoc networks. The nonuniform PSK constellations described in this dissertation have several advantages over nonuniform QAM, proposed in [20],

[25] for unequal error protection, for mobile wireless communication channels. For example, PSK constellations have constant envelopes, and knowledge of the received signal amplitude is not required for their demodulation. Such knowledge is required for optimum demodulation of QAM signals, but the received signal amplitude may be unknown and difficult to estimate. Thus, for mobile wireless communication, nonuniform PSK may often be more appropriate than QAM. Convolutional coding and nonuniform QAM constellations have also been investigated in [20], [25], where the goal is to provide unequal error protection for multiresolution source-encoded analog information. Li and Ephremides studied pulse amplitude modulation (PAM) and QAM for passive rate adaptation in the presence of channel fluctuation due to fading [30]. The goal of the work is the tradeoff between more reliable detection of fewer bits and less reliable detection of more bits.

Wireless network has become increasingly popular since their emergence in the 1970s. The ad hoc net work is one of the two variations of mobile wireless networks. The ad hoc network is infrastructureless and the other one is infrastructured. For an ad hoc network, all radios have mobility and can be connected dynamically in an arbitrary manner without the use of fixed routers. Interconnections between radios can be changed continuously. Characteristics of an ad hoc network such as arbitrary spatial distribution and dynamic connectivity result in communication link disparities that are exploited in the dissertation via simulcast signaling.

In the simulcasting schemes considered in this dissertation, some radios are more capable than other radios in that they can transmit two packets per slot instead of one, so it makes sense to have an unequal allocation of resources in the network to utilize this capability. The fairness of such an unequal allocation should be assessed. There are many approaches previously proposed for measuring fairness [12]–[14], [32]. The “Min-max index” [14] is a well known index for fairness which indicates evenness of a system, but it may not be good in indicating how the system uses available resources effectively when

different radios have resource utilizing capabilities. Recently, Dianati *et al.* proposed a "*Utility Fairness Index(UFI)*" in [13]. The UFI is parameterized to allow a trade-off between service fairness and effort fairness.

Various protocols for multipath routing has been researched [33]-[36]. Multipath routing exploits network resources effectively to maximize utilization. It reduces blocking probability and aggregates bandwidth on various paths so as to allow higher transmission rate to a network compared to single path [33]. In this dissertation, multipath routing is applied to exploit the simulcasting capability of radios on a route. By assigning higher transmission rates to routes with more simulcasting capability, the end-to-end throughput and delay can be improved.

Many researchers have investigated the optimal transmission range in ad hoc networks [37]-[43]. Kleinrock *et al.* [37], [38] interpret transmission power in an ad hoc network in terms of the number of neighbors of a radio and suggest a "magic number" of neighbors based on maximizing a packet's expected forward progress toward its destination. Their analysis indicates that a radio should transmit with a power so that the average number of neighbors within transmission range is six [37] or eight [38] to maximize overall network throughput. One of the critical assumptions in their analysis is that the network will not become disconnected because of power control. However, as the packet transmission power decreases, the number of neighbors of a radio decreases, and thus the network may have a high probability of becoming disconnected. Gupta and Kumar consider the effect of transmission power on connectivity and determine the critical power to guarantee connectivity of the overall network [42]. In [43], they show that if r is the range of transmission, then the relaying burden due to increment of the number of hops grows like $O(r^{-1})$, but the interference grows like $O(r^2)$. Thus, the net effect (the product) is a growth of $O(r)$. Their analysis implies that the smaller transmission power the better in terms of maximizing network throughput. However, if one chooses too small a range, then the network may loose connectivity. So, they

conclude that the optimal transmission power in an ad hoc network should be determined based on network connectivity.

Along with the optimal transmission range, energy efficiency is one of the key concerns in wireless communication systems. There has been a lot of research on transmission power control schemes over the past few years [44]-[50]. The chief motivation of these schemes is to mitigate the effect of interference that one user can cause to others. The results range from obtaining distributed power control algorithms to determining the information theoretic capacity achievable under interference limitations [51], [52]. Whereas most power control schemes aim at maximizing the amount of information sent for a given average power constraint, a recent study [53] considers minimizing the power subject to a specified amount of information being successfully transmitted. Rather than minimizing power, [54] considers the question of minimizing energy directly, and compares the energy efficiency, defined as the ratio of total amount data delivered and total energy consumed, of several medium access protocols.

CHAPTER 2
NETWORK MODEL AND PROTOCOLS FOR SIMULCASTING IN AD HOC NETWORKS

Before developing the application of simulcasting in ad hoc networks, we first provide an overview of the network model used in this research. The network model was chosen to be as fundamentally simple as possible, while still providing insight into the effects of using simulcasting. The system is a slotted transmission system, where we assume that all radios are perfectly synchronized. The packet arrival process is modeled by a Bernoulli random process. We assume that the radios have large packet buffers. Multiple access is provided by slotted-ALOHA [9].

Our physical-layer models are also selected to avoid obscuring the effects of simulcasting among other physical-layer phenomena. We begin by specifying some maximum transmission range at which a basic message can be received with a target error probability. Radios are considered to be neighbors if they are within that maximum transmission range. A packet collision occurs whenever a radio transmits a packet during a time slot and there is also a transmission by any of the neighbors of the packet's designated recipient. We assume that signals from radios that are not neighbors can neither be received nor cause a packet collision by interfering with transmissions from a radio's neighbors. Furthermore, we assume that all collisions result in packet errors and that there is immediate and perfect feedback on packets that collided or were otherwise received in error. Retransmissions occur after a back-off period that is chosen according to a geometric random variable, as discussed in Section 2.2.

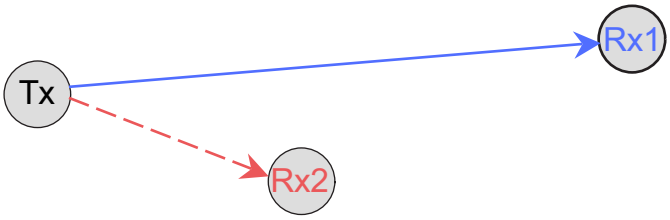

Figure 2–1. Simple scenario illustrating simulation at the link level.

2.1 Simulcast Transmission

Simulcasting has the potential to increase the average link throughput by allowing some radios to simultaneously transmit multiple packets to several different receivers while using approximately the same network resources as are required to transmit a single packet with unicasting. The easiest way to visualize this is in terms of propagation distance, which generally results in lower average received energy at the more-distant receivers. Figure 2–1 shows this in the case of two receivers.

Suppose that the power spectral density of the noise is the same at the two receivers and the only difference in received power is due to the difference in propagation distances. Then receiver 2 will be more-capable than receiver 1 in the sense that the higher signal-to-noise ratio at receiver 2 will allow it to successfully recover a message transmitted with a higher code rate or higher-order modulation than can be successfully recovered at receiver 1. Thus, in the terminology of [3]–[6], receiver 1 is a less-capable receiver, and receiver 2 is a more-capable receiver. By using unequal error-protection modulation or coding, each time that the transmitter sends a message to receiver1, it can include extra messages that can be recovered by receiver 2 because of its higher signal-to-noise ratio. In this case, the message intended for receiver 1 is called a basic message, and the messages intended for receiver 2 are called additional messages. We refer to these as the class of the messages.

Simulcast transmission can be achieve in many ways but depends on the ability to achieve a different level of error protection for the basic message than for the additional messages. One simple way that this unequal error protection can be achieved is through

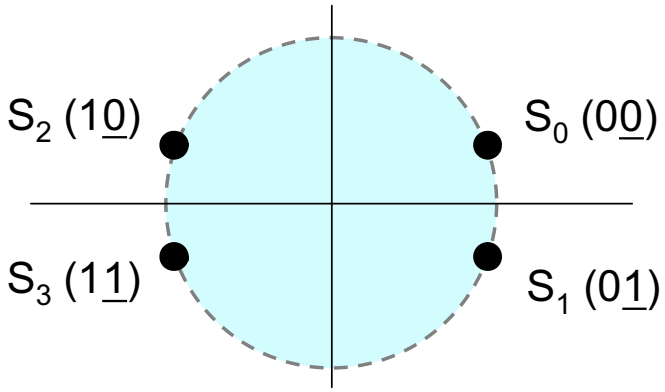

Figure 2–2. Nonuniform 4-PSK that achieves different levels of error protection for each bit.

nonuniform modulation [3], [4]. For instance, one of the simplest examples is the nonuniform quadriphase-shift key (QPSK) constellation illustrated in Figure 2–2.

For this constellation, the nonuniform spacing makes it much easier for a receiver to correctly recover the first bit than the second bit. Thus, the first bit can be used to send a basic message that is intended for a less-capable receiver or for all of a radio's neighbors, while the second bit is used to convey an additional message that can only be recovered by more-capable receivers. Thus, this technique can be used to simultaneously send two packets in a single slot, effectively doubling the link throughput. However, the use of this or any other simulcasting technique will result in some degradation in performance at the less-capable receiver if the transmit power is unchanged.

In [3], [4], two important parameters are introduced that provide a simple physical-layer characterization of simulcast transmission schemes that carry only two classes of messages. The parameters are the degradation and the capability disparity. Both of these parameters are typically specified in decibels. In general, these parameters must be specified in terms of the target error probabilities for the basic and additional messages. In this dissertation, the target error probabilities for these messages are assumed to be equal. By using a simulcast signaling scheme instead of a traditional signaling scheme that only conveys one basic message, the performance of the basic message

must be degraded. The degradation measures the additional amount of energy that must be received to achieve the same performance for the basic message with a simulcast signaling scheme as is achieved with a traditional signaling scheme. The capability disparity, or simply disparity, is a measure of how much more capable a receiver must be in order to recover an additional message in comparison to a receiver that only recovers the basic message. It can be calculated as the amount of additional energy that is required at a more-capable receiver to recover the additional message at the target error probability in comparison to the amount of energy required at a less-capable receiver to recover the basic message at the target error probability. In AWGN channel, for the same error probabilities for both of basic and additional message, the degradation and the disparity are given by for the offset angle θ [4]. Typical values for the degradation and disparity from [4] are 0.5 dB and 9.1 dB, respectively.

$$D_{dB}(\theta) = 20\log_{10}(\sec\theta), \tag{2–1}$$

$$\delta_{dB}(\theta) = 20\log_{10}(\cot\theta). \tag{2–2}$$

We begin by considering systems in which the transmit power is fixed, and the effects of this degradation on network performance are investigated. Furthermore, we initially assume that the simulcasting scheme is also not adapted to the network topology; in other words, the offset angle θ shown in Figure 2–2 is the same at all radios in the network. In Chater 6, we consider adaptation of the signal constellation shape along with the power in response to the channel conditions to the intended receivers. For most simulcasting techniques, when the offset angle θ is fixed, the performance degradation to the less-capable receivers can be made very small while still achieving a significant gain from transmissions to more-capable receivers. For example, if we consider only path loss for the transmission of a packet, by the definition of degradation and disparity, the transmission range for basic message, d_l, and additional message, d_m, are given simply

from the transmission range of unicasting, d_U, as

$$d_l(\theta) = d_U 10^{-D(\theta)/10n}, \quad (2\text{–}3)$$

$$d_m(\theta) = d_U 10^{-\delta(\theta)/10n}. \quad (2\text{–}4)$$

So, if the transmission range by unicasting, d_U, is $1,000m$ under the assumption that the propagation constant n is 4, we can gain $592.24m$ for the transmission range of additional message at the expense of just $28.37m$ reduction for the transmission range of basic message with 0.5 dB and 9.1 dB for values of the degradation and disparity, respectively. Further discussion and examples are given in Section 3.1.

In order to be able to demonstrate the advantages and disadvantages of simulcasting in the context of ad hoc networks, we employ the simple example of nonuniform QPSK described above for the remainder of this dissertation. With this scheme, each transmission can include at most two classes of message: a basic message packet and an additional message packet. All packets are assumed to be of the same length.

In the context of an ad hoc network, the concepts of more-capable and less-capable receivers must be extended, as each radio may act as a transmitter or receiver at different times. When a radio is acting as a receiver, its capability level will depend on its link (channel) from the transmitting radio. Therefore, we define the radio *links* as being more-capable or less-capable links. For the results presented in this paper, we assume that the only differences in link qualities are caused by differences in propagation distance. This also implies that links are symmetric, so if the link from radio 1 to radio 2 is a more-capable link, then so is the link from radio 2 to radio 1. Radios are able to discover the capabilities of neighboring radios during network maintenance or during regular packet transmission.

An example link map from our simulation is illustrated in Figure 2–3. Figure 2–3 shows the link capabilities for two different values of degradation and disparity, as explained below. The maps are based on typical degradation and disparity values from

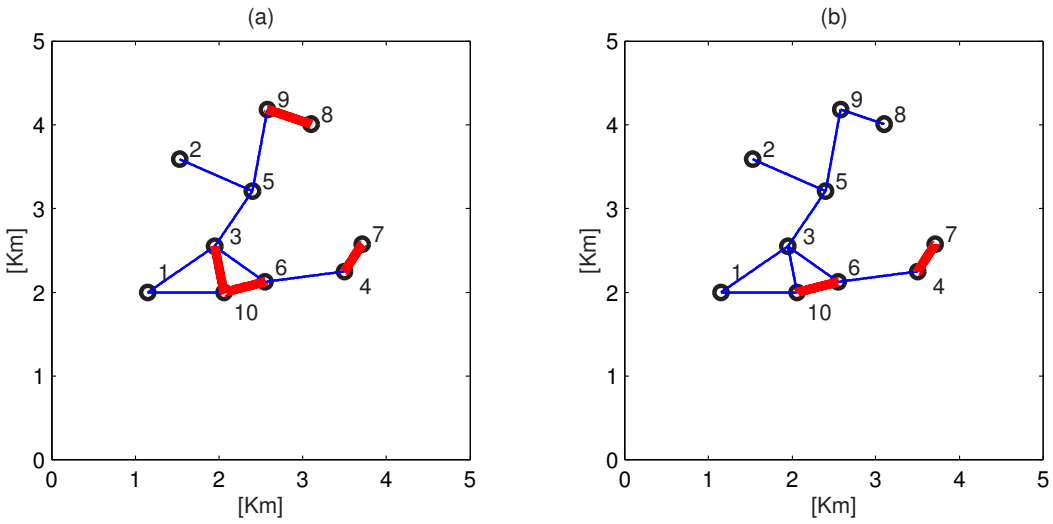

Figure 2–3. Link capabilities for a ten-node wireless network. Solid lines indicate less-capable links. Dashed lines are more-capable links. (a) NW1: For degradation of 0.5 dB and disparity of 9.1 dB (b) NW2: For degradation of 0.3 dB disparity of 11.4 dB.

[4] and exponential path loss proportional to the fourth power of distance. The figure illustrates the link capabilities for two scenarios: (a) NW1 is the case that $\theta = 19.25$ degrees, which yields a degradation of 0.5 dB and disparity of 9.1 dB, and (b) NW2 is the case that $\theta = 15$ degrees, which yields a degradation of 0.3 dB and disparity of 11.4 dB. The thin lines represent the less-capable links, and the thick lines represent the more-capable links. In scenario 2, NW2 has a more stringent requirement on the degradation, which results in a higher disparity. Thus NW1 has a larger number of more-capable links than NW2.

The use of simulcasting also causes some performance degradation to the less-capable links. For a fixed transmission power, the degradation results in the transmission range for the basic message being smaller for simulcasting than for unicasting. Thus, some links may break, which will cause two main effects to the network. First, a link may be critical to network connectivity, and when that link breaks, the network will become disconnected. Secondly, some routes may become longer because a node that is reachable in a single hop with unicasting may no longer be directly reachable. The increase in the

length of routes will reduce the end-to-end throughput. The expected number of links that break increases as the degradation increases, while the expected number of more-capable links increases as the degradation increases (and the required disparity decreases). Thus, the simulcast signaling scheme should be designed to ensure that the increase in link throughput from having a greater number of more-capable links translates into an increase in end-to-end throughput and that the impact on network connectivity is minimal. Results on this tradeoff are given in Sections 3.3 and 3.5.

As previously mentioned, we assume that the basic and additional messages require the same error probability. In fact, we consider a packet communication scheme in which any packet may be transmitted as either a basic or additional message, depending on the availability of more-capable links. The fact that a packet has been transmitted as one class of message over a link does not affect the class to which it will be assigned on later links. Thus, a packet may start out as an additional message, be transmitted as a basic message over some intermediate links, and be sent over the final link to its destination as an additional message. The only requirement that we place on the transmissions is that additional messages should be transmitted whenever possible in order to improve the network efficiency. This approach differs from the approaches in [3]–[6], in which nonuniform signaling techniques are used to transmit different classes of multimedia messages that may have different requirements on the packet error probability.

Each simulcast transmission contains two full packets, each of which has full headers. Thus, when a radio detects a packet, it will attempt to demodulate and decode the headers for both the basic and additional message. A receiver does not need to know *a priori* whether a packet contains an additional message; if no additional message is present, the receiver will not recover a valid header for that message (typically the CRC will fail). If neither of the packets is intended for a radio, then as usual, the radio can turn off its transceiver until the next slot to conserve energy. If either or both of the packets is intended for a radio, then they will be recovered in the usual way. We note that we

assume that all nodes will listen to the headers at the beginning of each slot. If a sleep schedule is employed to conserve energy at the radios, the performance of simulcasting may be significantly degraded by a reduction of receivers with more-capable links that are awake during any particular slot.

2.2 Medium Access Control

In the system that we consider, radios contend for the channel via slotted-ALOHA. We assume that the radios have long packet buffers such that every radio will always have a packet to transmit. When a radio suffers a collision, the radio will wait a random back-off time that is selected according to a geometric distribution. When a radio is successful in transmitting, it may immediately transmit in the following slot. For the system parameters that we consider, the performance is dominated by the effects of contention. Thus, the way that the probability of retransmitting in each slot (or equivalently, the average number of slots that the system will back off after a collision) is determined can have a significant effect on the performance of the system. For the results presented in the Chapter 3, each radio uses the same retransmission probability in any time slot. We show the simulcasting performance when we assign back-off time for retransmission unequally in Chapter 4. By adjusting this transmission probability, different average network attempt rates, G, can be obtained.

2.3 Routing Algorithm

In this dissertation, we consider a form of minimum-hop (min-hop) routing [31] in which the routing tables are modified to effectively utilize the capability of simulcasting. Our approach to including simulcasting in the network is designed to allow the transmission of an additional message whenever possible. As previously mentioned, we allow any packet to be sent as an additional message if an appropriate link is available. Whether a packet can be sent as an additional message at any node will depend on the packet's destination and the link capability of the next link on any minimum-hop route to that destination.

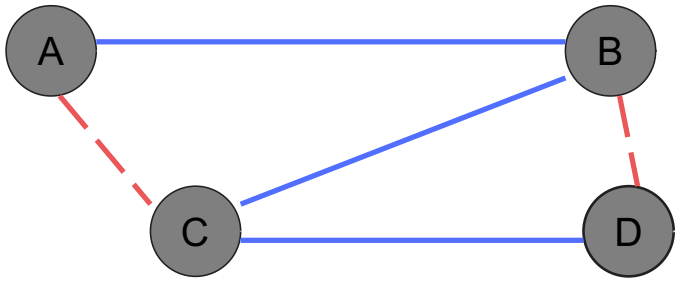

Figure 2–4. Example link map for a four-node wireless network.

Table 2–1. Routing table for radio A in Figure 2–4.

	Destination	Next Hop	No. of Hops
Normal Entires	B	B	1
	C	C	1
	D	B	2
Simulcast Enties	C	C	1
	D	C	2

The new routing tables are a superset of the standard min-hop routing tables. The standard min-hop routing table is always used for selection of the next-hop radio for the basic message. To this routing table is added a set of simulcast entries. For a routing table entry to be a valid simulcast entry, it must have a first hop that is a more-capable link and it must be a minimum-hop route. It is not required that the links after the first link be more-capable links. Thus, as previously mentioned, a packet that is transmitted as an additional message over one link may be transmitted as a basic message over other links, and vice versa.

To illustrate the modified routing table, consider the simple four-node network shown in Figure 2–4. In this figure, the more-capable links are shown as dashed lines, and the less-capable links are shown as solid lines. Table 2–1 shows example routing table for radio A. The routing table is formed as follows. The simulcast entries are specified first. Note that there will be no simulcast entry for destination radio B because there is no minimum-hop route for which the next hop from A is a more-capable link. However, there are simulcast entries for destination radios C and D. Both destinations C and D can

be reached in the minimum number of hops by first sending the packet over the more-capable link A to C. The routing table entries for the basic messages are labeled “Normal Entries” in Table 2–1 and are selected from the possible min-hop routes in the usual way. For the results presented in this section and Chapter 3, the normal and simulcast routing-table entries for a particular destination are allowed to be identical, even if other min-hop routes exist.

In Chapter 5, we consider how simulcasting impacts performance under multipath routing. Because radios that can simulcast a packet send more packets per transmission opportunity, it may be appropriate to route more packets along routes with more more-capable links.

2.4 Packet Selection Algorithm

The packet-selection algorithm should also be modified to ensure efficient use of the simulcasting capability. At each time that a radio transmits, it will attempt to utilize a more-capable link if one is available. By doing so, the link throughput can be increased because two packets are sent simultaneously by a radio in a single packet transmission interval whenever possible. An important feature of the simulcasting technique is that the basic and additional messages in a transmission do not have to have the same next-hop radio. Thus, for the network illustrated in Figure 2–4, radio A can simultaneously send a basic message to radio B and an additional message to radio C.

The packet-selection algorithm determines which packet(s) in a radio’s buffer will be transmitted in any given packet transmission interval. The packet-selection algorithm used in this dissertation is a modified first-in, first-out (FIFO) algorithm that ensures that more-capable links are utilized whenever possible. It functions in the following way. A radio that has at least one more-capable link will first try to select from its queue the first packet that can be sent as an additional message. This will not necessarily be the first packet in its queue. After the additional message (if available) is selected, then the first packet from the remaining set of packets will be sent as the basic message. In the absence

of mobility, packets intended for a particular destination will be transmitted in order, thereby minimizing the impact of simulcasting on the out-of-order arrival problem.

Table 2–2. Example packet buffer for radio A for network shown in Figure 2–4.

Packet ID	Destination
1	B
2	B
3	D
4	C

A brief example serves to illustrate this packet selection algorithm. Suppose that radio A's packet buffer contains four packets, as shown in Table 2–2. The first and the second column of the table show the packet IDs and the destinations of each packets, respectively. Then during the first interval in which radio A transmits, it first searches its buffer for the first packet that can be sent as an additional message. To do so, it compares the destination for each packet to the set of destinations in the simulcast entries in the routing table. In this case, the first packet that can be sent as an additional message is packet 3, which, based on the simulcast entry for destination D in Table 2–1, will be sent to next-hop radio C. Packet 1 is then selected for transmission as the basic message. So, when radio A transmits, it will simultaneously send messages to radios B and C using simulcast transmission. On radio A's next transmission, packet 4 will be selected as the additional message, and packet 2 will be sent as the basic message. Note that this simulcast transmission scheme is significantly different than multicasting that occurs at the network or application layers, in which one message is distributed to a group of different receivers. In simulcasting, multiple messages are simultaneously transmitted to a one or more neighbors of the transmitting radio.

CHAPTER 3
PERFORMANCE OF SIMULCASTING IN AD HOC NETWORKS WITH FIXED BACK-OFF ALGORITHM

In this chapter, we analyze the link and end-to-end throughputs for simulcasting in an ad hoc network. We consider a fixed network topology with a noise-free channel. Thus, for unicast signaling, the link throughput depends on the probability of collision and the time between transmission attempts, and end-to-end throughput depends on the link throughput and the number of hops the messages must travel. For simulcasting, these throughputs will also depend on the simulcasting parameters through the number of messages that can be sent as additional messages and the changes in the number of hops, which are caused by changes in the maximum transmission distance for the basic messages.

The analysis that follows is for three scenarios. In the first, the network topology is fixed, which allows the topological parameters to be easily calculated. In the second, N radios are uniformly distributed over an area A. Edge effects are neglected in the calculations. In the third scenario, the nodes are distributed according to a two-dimensional Poisson point process over an infinite plane.

3.1 Network Parameters

We begin by considering the effects of simulcasting on the network topology. In particular, we consider two network parameters that have a significant effect on the link and end-to-end throughputs. The first is the network degree, N_{deg}, which is the average number of neighbors of a radio. Here, we define a neighbor as any radio that is directly connected to the radio of interest by either a less-capable or more-capable link. The second parameter is R_m, which is the proportion of radios with more-capable links for fixed networks and the probability that a radio has at least one more-capable link for

random networks. For the network topology illustrated in Figure 2–3, $R_m = 7/10$ for $D = 0.5$ dB($\theta = 19.25$ degrees), and $R_m = 4/10$ for $D = 0.3$ dB ($\theta = 15$ degrees).

For our simple "good or bad" channel model, since the only factor that affects the signal-to-noise ratio is exponential path-loss (no random fading or shadowing is considered), whether two radios share a link depends only on the distance between the radios. Let d_U denote the maximum link distance for unicast signaling, and let $d_l(\theta)$ and $d_m(\theta)$ denote the maximum link distances for less- and more-capable links, respectively. These distances can be calculated as in Section 2.1,

$$\begin{aligned} d_l(\theta) &= d_U 10^{-D(\theta)/10n}, \\ d_m(\theta) &= d_U 10^{-\delta(\theta)/10n}, \end{aligned}$$

where $D(\theta)$ and $d(\theta)$ are the degradation and disparity (both in decibels), respectively. For nonuniform QPSK, these simplify to

$$\begin{aligned} d_l(\theta) &= d_U [\cos(\theta)]^{\frac{2}{n}}, \\ d_m(\theta) &= d_U [\sin(\theta)]^{\frac{2}{n}}, \end{aligned}$$

where n is the path-loss exponent. It is interesting to consider the coverage area of a transmitter, which is defined as the area of the region in which radios will have a link to that transmitter. Then the coverage areas for the basic and additional messages are given by $\pi {d_l}^2$ and $\pi {d_m}^2$, respectively. Consider the coverage area as a proportion of the coverage area for unicasting, $\pi {d_U}^2$. For $\theta = 10$ degrees, the proportions of coverage for the basic and additional messages are given by 0.985 and 0.174, respectively. Thus, for a reduction in coverage area of 1.5%, 17.4% of the coverage area supports more-capable links. If $\theta = 20$ degrees, the coverage area for the basic message is 6.0% less than that of unicasting, but the coverage area for the additional message is increased to 34.2% of unicasting. Thus, by appropriately choosing θ, the coverage area for additional message

transmission can be made reasonably large without significantly reducing the coverage area for the basic message.

Consider an arbitrary node in a network with nodes uniformly distributed over area A. Let p_l and p_m denote the probabilities that some other node is connected to that node by a less-capable link and more capable link, respectively. Then $p_l(\theta) \approx [d_l(\theta)]^2/A$, and $p_m(\theta) \approx [d_m(\theta)]^2/A$, where the approximations come from ignoring the edge effects of the finite area over which the nodes are placed. Then the network degree is given by

$$\begin{aligned} N_{deg}(\theta) &= (N-1)p_l(\theta) \\ &= (N-1)\frac{(\pi)[d_l(\theta)]^2}{A^2} \\ &= N_{deg}(0)[\cos(\theta)]^{4/n}. \end{aligned} \tag{3–1}$$

For the simulation results in Section 3.5, the transmission distance is close to the dimension of the simulation area, so the edge effect makes (3–1) yield inaccurate estimates if $p_l(\theta)$ and $d_l(\theta)$ are determined as specified above. However, we find that (3–1) gives a good approximation if the correct value of $N_{deg}(\theta)$ is found via simple topological simulation; therefore, we use this approach for the results in Section 3.5. The proportion of radios with more-capable neighbors can also be simply calculated by

$$R_m(\theta) = 1 - [1 - p_m(\theta)]^{(N-1)}.$$

Now consider an infinite network with nodes distributed in a plane according to a two-dimensional Poisson point process. Let λ denote the expected number of neighbors for unicasting. I.e., the expected number of radios in the area of size $\pi {d_U}^2$ is λ. Then for simulcasting with parameter θ, a radio is a neighbor of a particular radio if it is within distance $d_l(\theta) = d_U[\cos\theta]^{2/n}$. The neighbors of a radio lie within an area $\pi {d_U}^2[\cos\theta]^{4/n}$, and thus the number of neighbors is a Poisson random variable with expected value $N_{deg}(\theta) = \lambda[\cos\theta]^{4/n}$. Then, the probability that a radio has at least one more-capable

link is

$$\begin{aligned} R_m(\theta) &= P(\geq 1 \text{ neighbors in area } d_U^2(\sin\theta)^{4/n}) \\ &= 1 - P(\ 0 \text{ neighbors in area } \pi {d_U}^2(\sin\theta)^{4/n}) \\ &= 1 - e^{-\lambda(\sin\theta)^{4/n}}. \end{aligned}$$

3.2 Link Throughput

We apply the conventional techniques for link-throughput analysis of slotted ALOHA [9]. Let $E[D_i]$ be the expected value of the delay (in terms of number of slots) required for a packet transmitted by radio i to be successfully received by the designated next-hop radio. Then the link throughput at radio i, S_i, is defined by $S_i = 1/E[D_i]$. The average link throughput for a network of N nodes is given by

$$S = \frac{1}{N}\sum_{i=1}^{N} S_i. \tag{3–2}$$

We evaluate (3–2) for two different scenarios. In unicast transmission, simulcasting is not allowed, and each radio sends at most one packet to one next-hop radio during a time slot. For simulcast transmission, two packets can be sent simultaneously by a radio during a time slot if that radio has any more-capable links, as described in Section 2.1. The link throughputs for unicast and simulcast transmission are denoted by S_U and S_S, respectively.

The link throughput will depend on several parameters. Define G_i to be the attempt rate of the ith radio. Let $S_{U,i}$ and $S_{S,i}(\theta)$ be the link throughput at radio i for unicast and simulcast transmission with phase offset θ, respectively. The throughput at radio i depends on the number of neighbor radios $B_i(\theta)$, the probability of collision $C_i(\theta)$, and the retransmission rate for unsuccessful packets $R_i(\theta)$.

3.2.1 Unicast Transmission

For unicast transmission, a radio sends only a single message in a slot, and that message is intended for only one of its neighbors. In this case, the throughput for the ith

radio can be determined as follows. The attempt rate must satisfy $G_i = S_{U,i} + R_i$, where $R_i = G_i C_i$. Then the throughput is given by

$$S_{U,i} = G_i(1 - C_i), \tag{3–3}$$

where, if radio i has B_i neighbors and G is the average attempt rate over all radios, then

$$C_i \approx \frac{1}{B_i} \sum_{j=1}^{B_i} C_{i,j}. \tag{3–4}$$

Here $C_{i,j}$ is the probability of collision at the jth neighbor of radio i, which is given by

$$C_{i,j} \approx 1 - (1 - G)^{B_{i,j}}, \tag{3–5}$$

where $B_{i,j}$ is the number of neighbors of the jth neighbor of radio i. The result in (3–4) is approximate because it assumes equal probability of transmission to each neighbor, and (3–5) is approximate because the offered load from the potential interferers is replaced by the average offered load. The average link throughput S_U can be approximated by using (3–3)-(3–5) in (3–2).

3.2.2 Simulcast Transmission

We consider the link throughput of simulcasting using nonuniform QPSK with parameter θ. First consider the throughput for the basic message. Although the number of neighbors that can be reached by direct transmission is reduced, the interference range stays constant. Thus the link throughput for the basic message will be approximately equal to the link throughput for unicasting, $S_{U,i}$. Now consider the additional message. For the case of long packet buffers, if the packet generation rate is sufficiently high then a radio that has a more-capable link will always have a packet that can be sent as an additional message. Then the link throughput for the ith radio with simulcast transmission, $S_{S,i}(\theta)$ can be approximated as $S_{S,i}(\theta) \approx 2S_{U,i}$ if radio i has a more-capable link and $S_{S,i}(\theta) = S_{U,i}$, otherwise. For a network of N nodes, and let $M(\theta, i)$ be an indicator function such that $M(\theta, i) = 1$ if radio i has a more-capable link and

$M(\theta, i) = 0$ otherwise. Then the throughput for simulcast transmission for the fixed network can be approximated by

$$S \approx \frac{1}{N} \sum_{j=1} [2S_{U,i} M(\theta, i) + S_{U,i}(1 - M(\theta, i))], \tag{3–6}$$

and for the random network,

$$\begin{aligned} S &\approx E[S_{U,i} M(\theta, i) + S_{U,i}(1 - M(\theta, i))] \\ &= S_{U,i}[1 + R_m(\theta)]. \end{aligned} \tag{3–7}$$

So for long packet buffers and high packet generation rates, simulcast transmission has the capability to improve the link throughput by a factor of up to $R_m(\theta)$. However, it is not clear that this increase in link throughput will translate into a corresponding increase in end-to-end throughput. This is the topic of the next subsection.

3.3 End-to-end Throughput

We consider the end-to-end throughput for simulcasting as a function of θ. Then the end-to-end throughput for unicasting can be found by setting $\theta = 0$. The end-to-end throughput over T time slots is defined by

$$S_{ete} \approx \frac{N_D(T)}{T},$$

where $N_D(T)$ is the number of packets that reach their final destination in T time slots. We are interested in steady-state conditions and consider the expected value of S_{ete}, which is not a function of T. Consider a generic route, as shown in Figure 3–1.

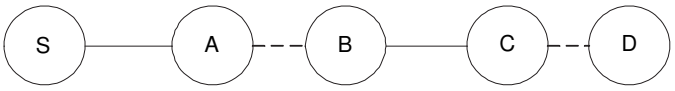

Figure 3–1. Example route for estimating end-to-end throughput.

We analyze the throughput by considering the delay required to transmit two packets (corresponding to the two types of messages) over such a route. Under the best-case

scenario, one of the packets can be sent as an additional message over each of the more-capable links (shown as dashed lines). Then for each less-capable link (shown as solid lines), the expected delay is $2E[Di]$ for the two packets. For each more-capable link, the expected delay is only $E[Di]$ for the two packets. Thus for the example in Figure 3–1, the expected delay for both packets to reach the destination (not counting queuing delays) is $6E[D]$, where $E[D]$ is the expected delay at an arbitrary node. Then the average end-to-end throughput for each packet is

$$S_{ete} \leq \frac{2}{6E[D]} \approx \frac{S_U}{3}.$$

Let $H(\theta)$ be a random variable representing the number of hops in an arbitrary route. Note that as θ changes, the distribution of H changes, as discussed in Section 2.1. Then in general, the end-to-end throughput can be approximated by

$$S_{\text{ete}} \approx \sum_{i=1}^{N} \frac{2P(H(\theta)=i)}{iR_m(\theta)E[D] + 2i[1-R_m(\theta)]E[D]}. \tag{3–8}$$

This expression is approximate because the distribution of the number of hops for the packets that take a more-capable link may be different than for the packets that do not take any more-capable link. For instance, more-capable links may be used more often than less-capable links to transmit a packet to its destination.

Note also that $S_{ete}(\theta)$ is a non-linear function of $R_m(\theta)$. Unlike the link throughput, the end-to-end throughput does not increase in direct proportion to $R_m(\theta)$. Note that the summation term will decrease as θ and $R_m(\theta)$ increase, as the number of hops increases. Then if the distribution of the number of hops is constant, a 50% increase in end-to-end throughput requires at least $R_m(\theta) = 2/3$. For θ large enough to satisfy this requirement, the expected number of hops may be significantly larger than for unicasting, thereby reducing the gain from the increase in link throughput.

We investigate the value of θ that maximizes S_{ete} by estimating the distribution of $H(\theta)$ via empirical and analytical distributions. The results using the empirical

distribution are given in Section 3.5. Here we investigate the performance under two simple analytical distributions for $H(\theta)$.

Consider a network of radios distributed according to a Poisson point process over a plane. Consider first the distribution for $H(0)$, the number of hops in a route when unicasting is employed. We wish to use distributions such that:

1) $\exists\, k \ni \forall\, i > \ k, j > k$, $P(H(0) = i) > P(H(0) > j)$ for all $i < j$, and

2) $P(H(0) = i) > 0$, i=1,2,...

The first criterion provides locality. Beyond some local neighborhood, it is more likely for a packet to have a closer destination than one further away. The second criterion allows any radio in the network (other than the source) to be a destination for the packet.

We first analyze the performance for a geometric distribution for the number of hops. Suppose first that $H(0)$ has geometric distribution with parameter α, and let $\bar{H} \ = \ E[H(0)]$,

$$P(H(0) = i) = \begin{cases} \alpha(1-\alpha)^{i-1}, & \text{i=1,2,....} \\ 0, & \text{otherwise.} \end{cases}$$

Then, the distribution of $H(\theta), 0 < \theta \leq 45$ degrees, should be geometric with parameter $\beta(\theta)$, $\beta(\theta) < \alpha$. To determine a reasonable estimate for $\beta(\theta)$, consider the probability of having a 1-hop route for unicasting $P(H(0) \ = \ 1) \ = \ \alpha$. The probability that the destination radio is still within communication range when simulcasting is employed is $(\pi d_l^2)/(\pi d_U^2) \ = \ (\cos\theta)^{4/n}$. There are four cases to consider for a particular link along a route in going from $\theta = 0$ to $\theta > 0$:

1) The link is still within communication range, so the route is not affected.
2) The link is not within communication range, but another link can be used to achieve the same number of hops in the route.
3) The link is not within communication range and so the number of hops in the route increases by one.

4) The link is not within communication range and that link failure requires significant rerouting, resulting in the number of hops in the number of hops in the route increasing by more than one.

Based on the probability of being able to reach the same 1-hop destination above, we model $H(\theta)$ as a geometric random variable with parameters $\beta(\theta) = \alpha(\cos\theta)^{4/n}$. This most accurately models cases 1 and 3 above. We note also that cases 2 and 4 will have opposite effects on $H(\theta)$, so this model seems reasonable, if perhaps a bit optimistic because of the large impact of case 4. For this distribution $E[H(\theta)] = \bar{H}(\cos\theta)^{-4/n}$.

For the infinite network, $R_m(\theta)$ is the probability that a radio has at least one more-capable link and is given by

$$R_m(\theta) = 1 - Pb(0 \text{ radios in area } \pi d_U^2(\sin\theta)^{4/n})$$

Let $\lambda' = (\sin\theta)^{4/n}\lambda$. Then, as previously calculated the proportion of the radios with more-capable link(s) $R_m(\theta)$ in Section 3.1,

$$\begin{aligned} R_m(\theta) &= 1 - e^{-\lambda'} \\ &= 1 - e^{-\lambda(\sin\theta)^{4/n}}. \end{aligned} \tag{3–9}$$

The average end-to-end throughput can then be approximated by

$$S_{ete} \approx \frac{S_U}{1 - 0.5[1 - e^{-\lambda(\sin\theta)^{4/n}}]} \sum_{i=1}^{\infty} \frac{\alpha(\cos\theta)^{4/n}[1 - \alpha(\cos\theta)^{4/n}]^{i-1}}{i}. \tag{3–10}$$

From [55],

$$\ln(1+z) = z - \frac{1}{2}z^2 + \frac{1}{3}z^3 - \frac{1}{4}z^4 + ...$$

Then,

$$\ln\left(\frac{1}{q}\right) = \sum_{i=1}^{\infty} \frac{(1-q)^i}{i}. \tag{3–11}$$

Letting $q = \alpha(\cos\theta)^{4/n}$ and using (3–10) and (3–11) yields

$$S_{ete} \approx \frac{S_U}{1 - 0.5[1 - e^{-\lambda(\sin\theta)^{4/n}}]} \frac{\alpha(\cos\theta)^{4/n}}{1 - \alpha(\cos\theta)^{4/n}} \ln\left[\frac{1}{\alpha(\cos\theta)^{4/n}}\right]. \quad (3\text{–}12)$$

Although (3–12) is too complicated to allow the maximum value to be found via direct analysis, the maximum value can easily be found via numerical methods.

The results of this numerical optimization are shown in Figures 3–2–3–4 for $n = 2$ and in Figures 3–5–3–7 for $n = 4$. The results in Figures 3–2–3–4 are for $\bar{H} = \frac{1}{\alpha}$ is equal to 2, 4, and 8, respectively, as are the results in Figures 3–5–3–7. The graphs labeled (a) illustrate G_{ete}, the maximal gain in the end-to-end throughput from using simulcasting instead of unicasting, $G_{ete}(\theta) = S_{ete}(\theta)/S_{ete}(0)$. The graphs labeled (b) illustrate the values of θ that maximizes G_{ete}, which is defined as optimal offset angle θ_o. The results indicate that the expected gain in the end-to-end throughput for simulcasting varies from 20.9% to 62.2% for $n = 2$ and from 60.1% to 90.0% for $n = 4$, where λ varies from 4 to 12. The maximum gains from simulcasting are achieved when the distributions favors shorter routes ($\frac{1}{\alpha} = 2$) and larger number of neighbors ($\lambda = 12$). This is reasonable because the impact of simulcasting on increasing route length will be smallest when the routes are shortest for unicasting under assumption of full connectivity of network. When λ is large, the probability of having a more-capable neighbor increases, and thus more radios can transmit two messages in each interval. The simulcasting gain is greater for $n = 4$ than $n = 2$ because of the way that the exponential path loss translates differences in energy into differences in distance. The energy for the basic and additional messages scale as $\cos^2\theta$ and $\sin^2\theta$, respectively. However, the coverage areas for the basic and additional messages scales as $(\cos\theta)^{4/n}$ and $(\sin\theta)^{4/n}$, respectively. Consider $\theta = 30$ degrees. For $n = 2$, the coverage areas for the basic and additional messages are 75% and 25%, respectively, of that for unicasting. For $n = 4$, the coverage areas for the basic and additional messages are 86.6% and 50%, respectively, of that of unicasting. Thus for

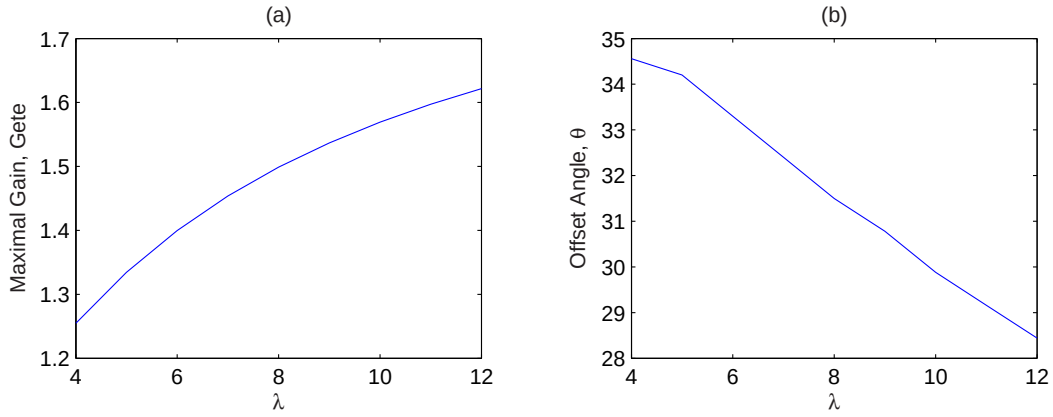

Figure 3–2. (a) Maximal gain in end-to-end throughput, G_{ete}, and (b) optimal offset angle(degree), θ_o, to maximize G_{ete}, at $\frac{1}{\alpha} = 2$, and $n = 2$.

$n = 4$, the coverage areas for both the basic and additional messages are significantly greater than for $n = 2$ at the same value of θ.

The θ_o varies from 27.5 degrees to 34.5 degrees for $n = 2$ and from 18.9 degrees to 32.2 degrees for $n = 4$. It decreases as λ increases. That is, the θ_o is maximum for distributions favoring shorter routes and fewer neighbors and is minimum for distributions favoring longer routes and many neighbors. It means that, as we discussed, under the assumption of full connectivity of network, the effect of increasing route length by employing simulcasting is larger with longer routes. Having more neighbors increases the probability of being able to perform simulcasting for even small θ. So, in order to maximize the end-to-end throughput, smaller θ is required to avoid increasing route length by employing simulcasting as the number of neighbors increases.

Figures 3–8 and 3–9 show the maximum end-to-end throughputs versus θs for various λs at $n = 2$ and $n = 4$, respectively, over the attempt rate G of 0 to 1 with $\bar{H} = 4$. The unicasting throughput S_U is assumed as unity in this results. As λ increases from 4 to 12, the θ_m which maximizes the maximum end-to-end throughput decreases from of 35 to 25 and from 30 to 15 degrees for $n = 2$ and $n = 4$, respectively. For $n = 4$, the value of θ_o is smaller and decreases in a larger range as λ increases compared to for $n = 2$. In other words, for $n = 4$, θ_o is more sensitive to λ compared to for $n = 2$. This is because,

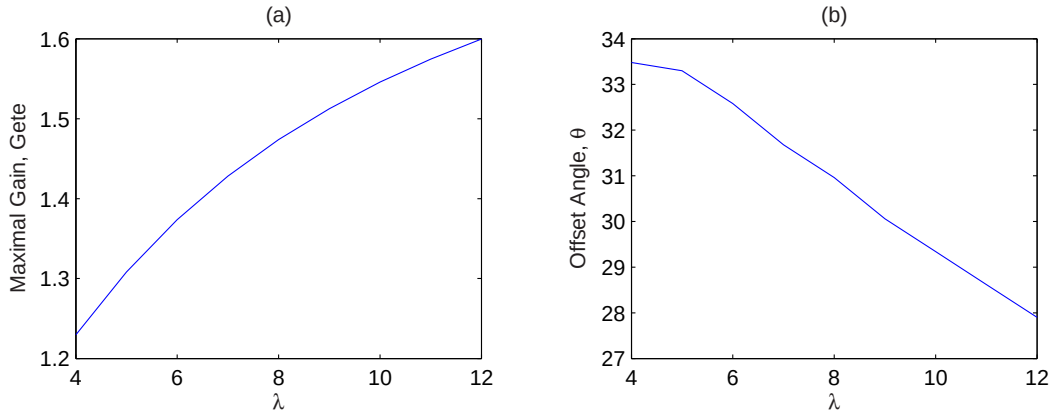

Figure 3–3. (a) Maximal gain in end-to-end throughput, G_{ete}, and (b) optimal offset angle(degree), θ_o, to maximize G_{ete}, at $\frac{1}{\alpha} = 4$, and $n = 2$.

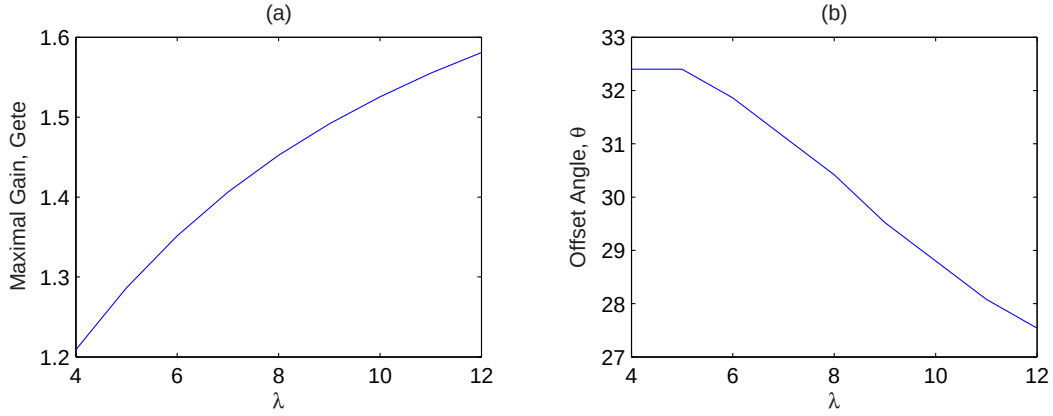

Figure 3–4. (a) Maximal gain in end-to-end throughput, G_{ete}, and (b) optimal offset angle(degree), θ_o, to maximize G_{ete}, at $\frac{1}{\alpha} = 8$, and $n = 2$.

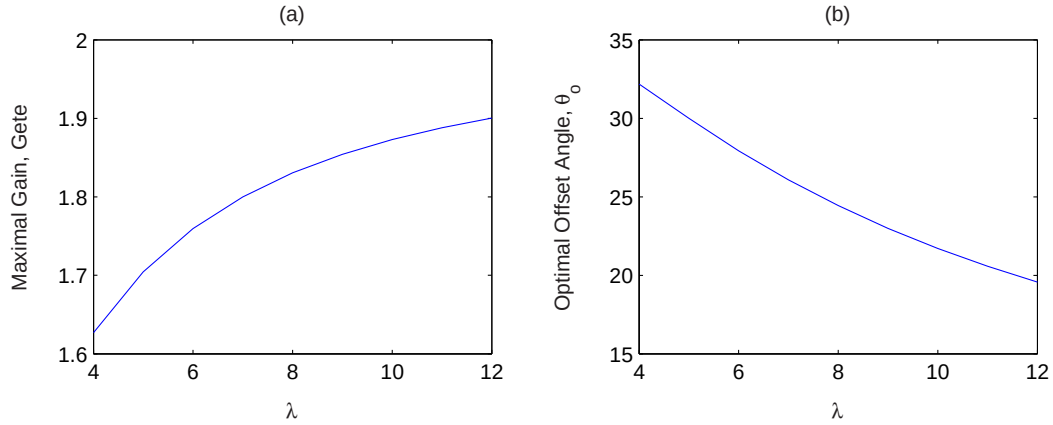

Figure 3–5. (a) Maximal gain in end-to-end throughput, G_{ete}, and (b) optimal offset angle(degree), θ_o, to maximize G_{ete}, at $\frac{1}{\alpha} = 2$, and $n = 4$.

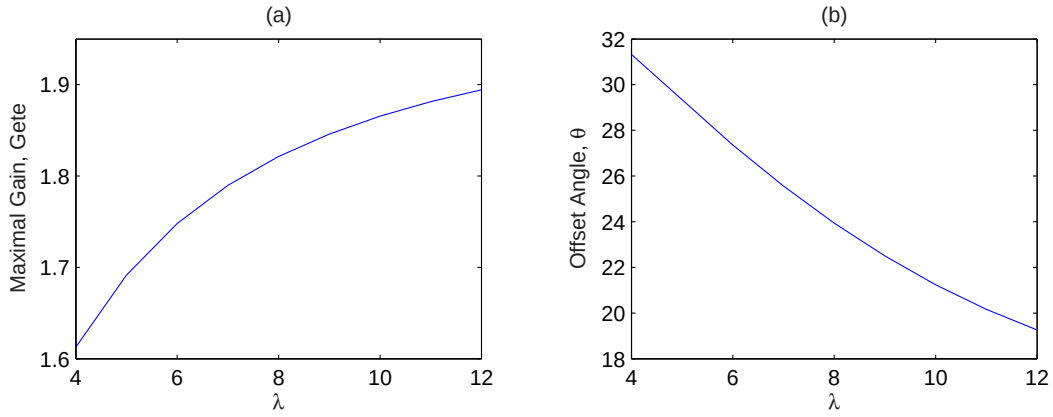

Figure 3–6. (a) Maximal gain in end-to-end throughput, G_{ete}, and (b) optimal offset angle(degree), θ_o, to maximize G_{ete}, at $\frac{1}{\alpha} = 4$, and $n = 4$.

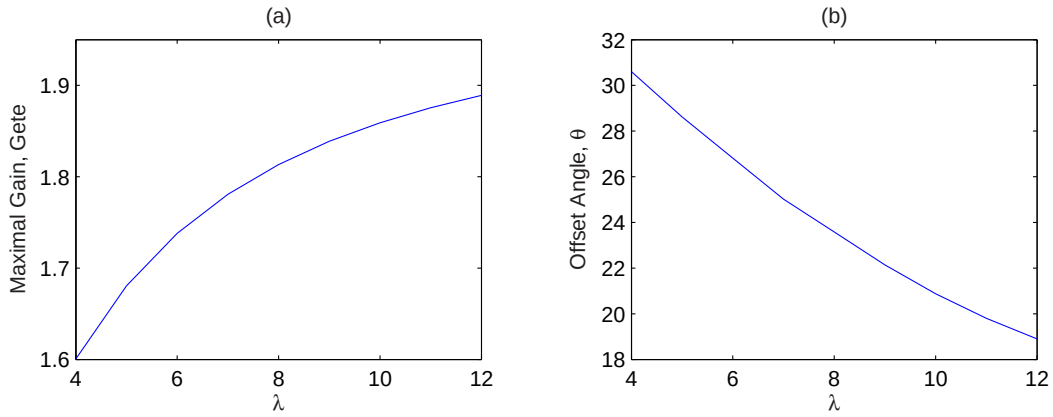

Figure 3–7. (a) Maximal gain in end-to-end throughput, G_{ete}, and (b) optimal offset angle(degree), θ_o, to maximize G_{ete}, at $\frac{1}{\alpha} = 8$, and $n = 4$.

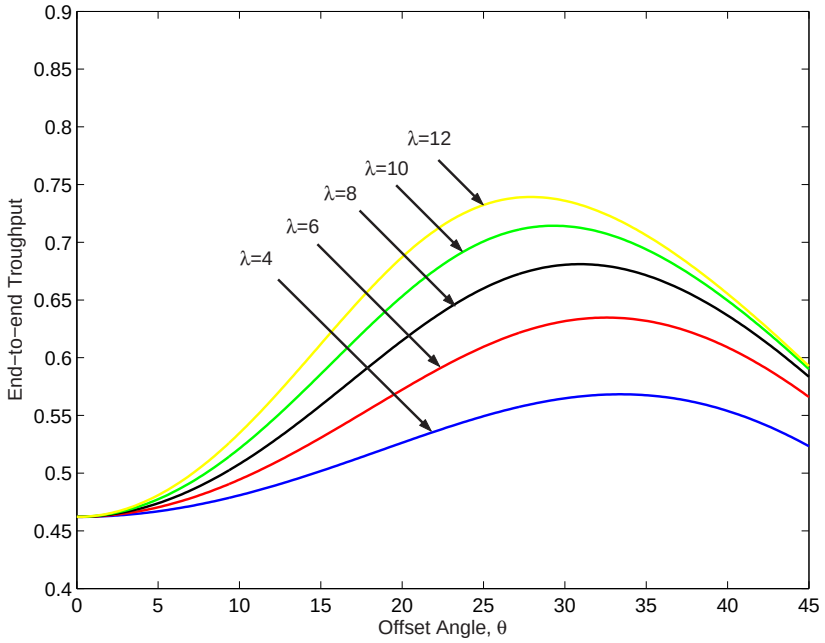

Figure 3–8. The maximum end-to-end throughputs for simulcasting with various network density λs in geometric distribution for the number of hops, at the expected value of the number of hops $\frac{1}{\alpha} = 4$, and propagation constant $n = 2$.

at a same value of θ, the coverage areas for both of basic and additional messages when simulcasting is employed are greater for $n = 4$ than for $n = 2$, and when λ is large, the probability of having a more-capable neighbor increases.

The Maximum end-to-end throughput increases from 0.55 to 0.73 and from 0.72 to 0.87 for $n = 2$ and $n = 4$, respectively, as λ increases from 4 to 12. Note that in Figures 3–8 and 3–9, for n=4, the maximal end-to-end throughput achieved is greater compared to for $n = 2$ as previously discussed.

The second distribution that we consider for the number of hops is a modified Poisson distribution. The Poisson distribution has probability mass at zero, which is undesirable for our application, so we let $H(0) - 1$ be Poisson with expected value γ. Then,

$$P(H(0) = k) = \begin{cases} e^{-\gamma}\frac{\gamma^{k-1}}{(k-1)!}, & \text{k=1,2,....} \\ 0, & \text{otherwise,} \end{cases}$$

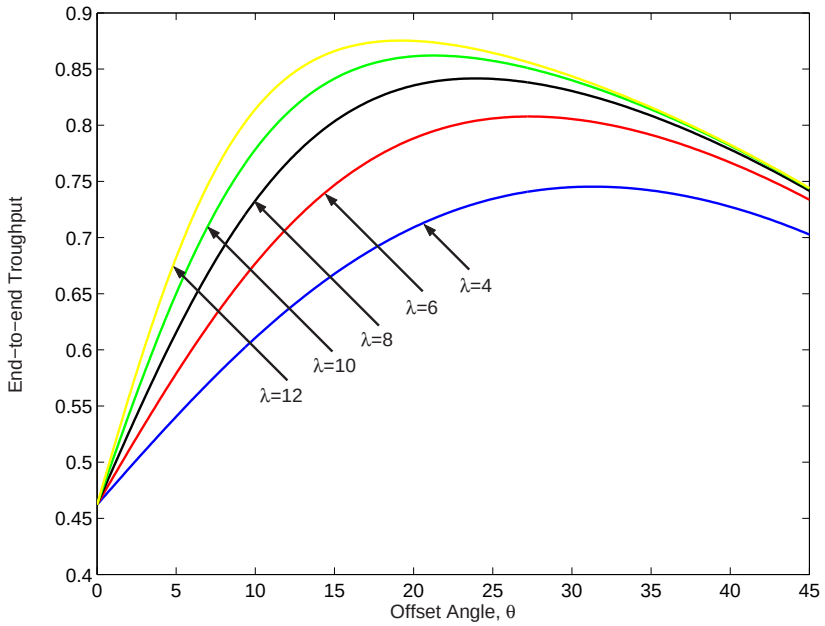

Figure 3–9. The maximum end-to-end throughputs for simulcasting with various network density λs in geometric distribution for the number of hops, at the expected value of the number of hops $\frac{1}{\alpha} = 4$, and propagation constant $n = 4$.

and $\bar{H} = \lambda + 1$. Following similar argument as for the geometric distribution, we let $H(\theta) - 1$ be Poisson with expected value of $\gamma(\theta)$ given by $\gamma/(\cos\theta)^{4/n}$. As for the geometric distribution, $E[H(\theta)] = \bar{H}(\cos\theta)^{-4/n}$. The average end-to-end throughput can then be approximated by

$$S_{ete} = \frac{S_U e^{-\gamma(\theta)}}{1 - 0.5[1 - e^{-\lambda(\sin\theta)^{4/n}}]} \sum_{k=1}^{\infty} \frac{\gamma(\theta)^{k-1}}{k(k-1)!}.$$

Note that

$$\sum_{i}^{\infty} \frac{\gamma(\theta)^{k-1}}{k(k-1)!} = \frac{1}{\gamma(\theta)} \sum_{k=1}^{\infty} \frac{\gamma(\theta)^{k}}{k!} = \frac{e^{\gamma(\theta)}}{\gamma(\theta)}.$$

Thus,

$$S_{ete} = \frac{S_U}{1 - 0.5[1 - e^{-\lambda(\sin\theta)^{4/n}}]\gamma(\theta)},$$

and

$$G_{ete} = \frac{S_{ete}(\theta)}{S_{ete}(0)} = \frac{(\cos(\theta))^{4/n}}{1 - 0.5[1 - e^{-\lambda(\sin(\theta))^{4/n}}]}.$$

Note that, for the Poisson distribution for the number of hops, the simulcasting gain is independent on the average number of hops.

Figures 3–10 and 3–11 show the analytical results for the end-to-end throughput of simulcasting under the Poisson distribution for the number of hops for $n = 2$ and for $n = 4$, respectively. The graphs labeled (a) illustrate G_{ete}, and the graphs labeled (b) illustrate the values of θ_o according to various network densities.

The results indicate that the expected gain in the end-to-end throughput for simulcasting varies from 10.0% to 46.4% for $n = 2$, and from 53.1% to 86.1% for $n = 4$ for λ in the range of 4 to 12. The maximum gains from simulcasting are achieved when the distributions favors larger number of neighbors ($\lambda = 12$) as the case of geometric distribution, but the gains are 5% to 10% smaller than for the geometric distribution. This is reasonable because the Poisson distribution has lower probability of choosing shorter routes than the geometric distribution, which significantly impacts on the end-to-end throughput. The simulcasting gain is also greater for $n = 4$ than $n = 2$ for the same reason described for the geometric distribution.

The θ_o varies from 25.3 to 27.8 degrees for $n = 2$ and from 26.7 to 17.3 degrees for $n = 4$. These values are about 5 degrees smaller than for the geometric distribution for both of $n = 2$ and $n = 4$. The intuitive explanation is that the effect of increasing route length by employing simulcasting with relatively large θ is more significant for the Poisson distribution.

Mostly, the θ_o decreases as λ increases. However, notice that θ_o is no-monotonic for $n = 2$. This is because the probability of choosing a short route is low for the Poisson distribution. For the geometric distribution, θ_o is maximal with the shortest routes and the

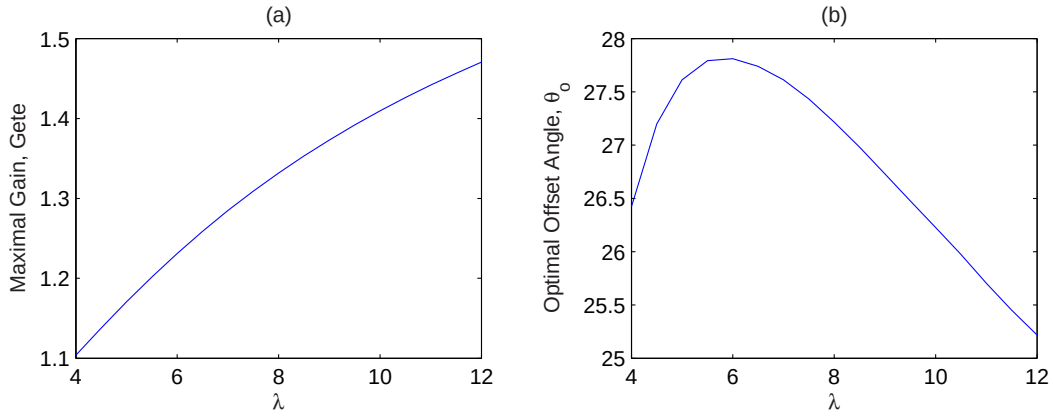

Figure 3–10. (a) Maximal gain in end-to-end throughput, G_{ete}, and (b) optimal offset angle(degree), θ_o, to maximize G_{ete}, at $n = 2$.

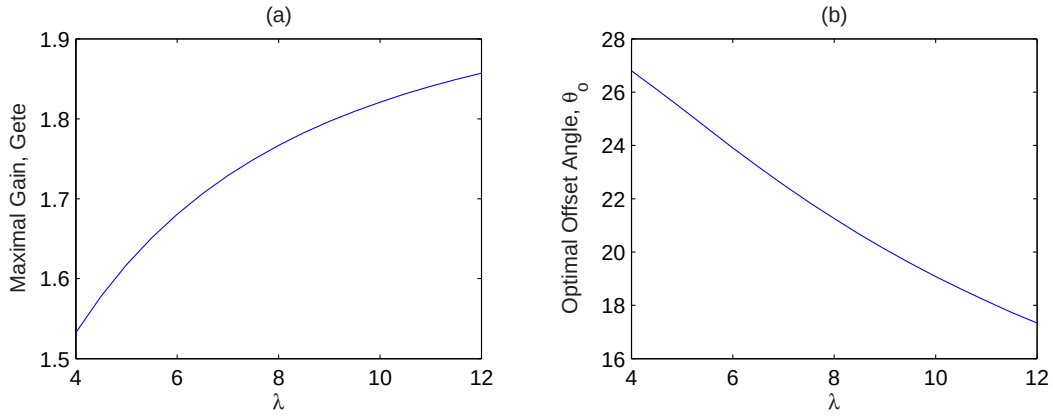

Figure 3–11. (a) Maximal gain in end-to-end throughput, G_{ete}, and (b) optimal offset angle(degree), θ_o, to maximize G_{ete}, at $n = 4$.

fewest neighbors because the effect of increasing route length by employing simulcasting is less with shorter routes and with fewer neighbors, under the assumption of full network connectivity. However, for the Poisson distribution, the effect increases route length when simulcasting is used with a small number of neighbors because of the smaller probability of choosing a short route. For $n = 2$, it is more apparent because the probability that the destination radio is still within communication range when simulcasting is employed $(\cos\theta)^{4/n}$ is smaller for $n = 2$ than for $n = 4$.

Figures 3–12 and 3–13 show the maximum end-to-end throughputs for simulcasting in Poisson distribution for the number of hops according to various θs along with various

λs for $n = 2$ and $n = 4$, respectively, over the G of 0 to 1 with $\gamma = 4$. The unicasting throughput S_U is assumed as unity as of geometric distribution case.

As λ increases from 4 to 12, the θ_m which maximizes the maximum end-to-end throughput decreases from 25 to 30 and from 15 to 25 degrees for $n = 2$ and $n = 4$, respectively. As the geometric distribution, for $n = 4$, the end-to-end throughput is more sensitive to λ compared to for $n = 2$. The maximal end-to-end throughput ranges from 0.33 to 0.46 and from 0.33 to 0.58 for $n = 2$ and $n = 4$, respectively. The overall pattern is similar and can be explained with the same reason as for the geometric distribution case.

In comparison with the geometric distribution, for the Poisson distribution, the achieved maximal end-to-end throughputs and the values of θ_o to achieve them are less and the range of θ_o over the domain of λ is relatively smaller. As previously discussed, it is because the Poisson distribution has lower probability of choosing short routes and the variation of Poisson distribution is less than for the geometric distribution. Based on the analysis and the numerical results of the end-to-end throughput, if the number of hops follows the geometrical distribution, a higher end-to-end throughput is expected, and if the number of hops follows the Poisson distribution, a relatively stable end-to-end throughput is achieved.

3.4 Mobility

The mobility model is an important issue in the study of mobile ad hoc networks. Recent studies [56]-[59] report that in simulations of mobile ad hoc networks, the probability distribution governing the movement of the nodes typically varies over time and converges to a “steady-state”, or stationary distribution.

Thus a simulation of a network of mobile radios often experiences a transitory period before conveying to the steady state. One approach to deal with the fluctuating conditions is to throw away the simulation data for some initial time period. A more efficient alternative is to choose the initial locations and speeds of the radios from the

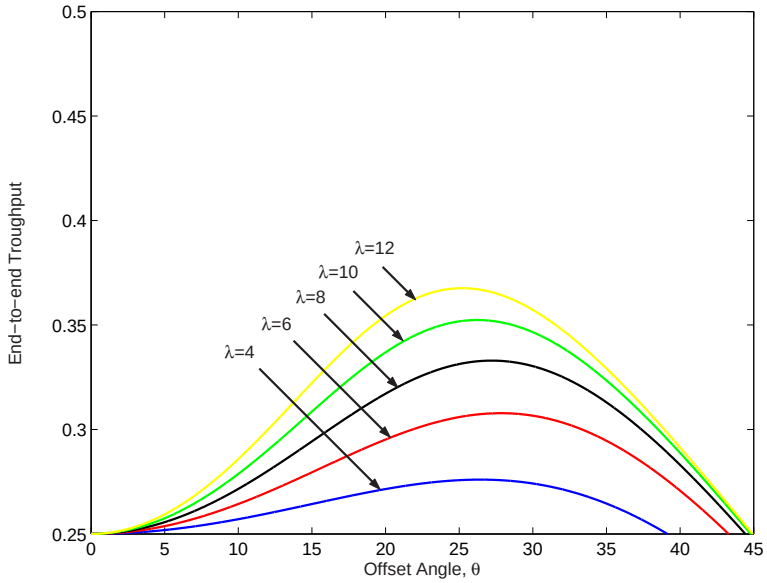

Figure 3–12. The maximum end-to-end throughputs for simulcasting with various network density λs in Poisson distribution for the number of hops, at the expected value of the number of hops $\gamma = 4$ and propagation constant $n = 2$.

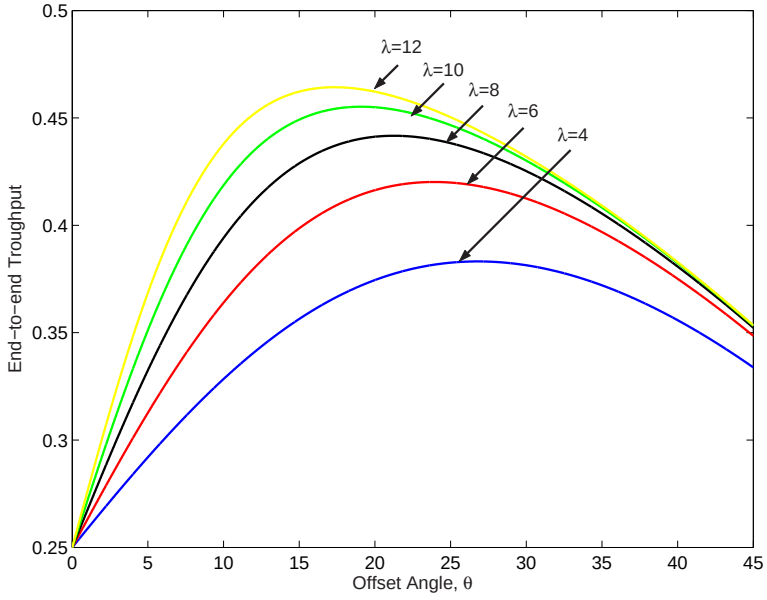

Figure 3–13. The maximum end-to-end throughputs for simulcasting with various network density λs in Poisson distribution for the number of hops, at the expected value of the number of hops $\gamma = 4$ and propagation constant $n = 4$.

stationary distributions for the mobility model so that convergence is immediate and no data needs to be discarded. However, because the initial location and speeds with stationary distributions bring a centralized shape of distribution (the most convergent speeds and the locations are gathered at a certain range of speed and location), it is hard to see the effects of mobiles moving around in a large area. The uniformly distributed "steady-state" needs to be studied.

We use the random waypoint mobility model, which is one of the most popular mobility models for communication networks, for our simulation. In this model, an initial point p_0 and a destination point p_1 are assigned uniformly in the area A, and speed is assigned to a mobile at the inital point uniformly in an arbitrary range of speed. The initial and destination points are chosen independently. Once the mobile reaches the destination, a new destination is chosen uniformly, independently of all previous destinations and speeds. Mobiles may pause when it reaches each destination, or they may immediately move to the next destination without pausing. If they pause, the pause times are chosen independently of speed and location.

The random waypoint model is a commonly used mobility model in the simulation of ad hoc networks. However, it has problems such as the decay of average speeds as the simulation progresses, a difference between the initial and the final nodes distribution. It is known that the spatial distribution of network nodes moving according to this model is, in general, nonuniform. For example, with this model, a mobile spends more time at lower speed, therefore it is more likely to be sampled at low speed. The initial mobile position is uniform in the area A, however, with time, the distribution of mobile positions tends to be more dense towards the middle of the area.

To overcome the problems of random waypoint model, J. Le Boudec [59] recently presented how to obtain the stationary distribution of location and speeds for the simulation of mobility model based on palm caculus. By palm calculus, the histogram of the terminating or non-terminating ergodic simulation can be predicted. It is applied to the

random waypoint model to achieve an initial distribution equal to the stationary distribution of random waypoint. Simply, how to generate the stationary distribution of the previous and next waypoint and the current mobile position can be obtained as follows. Let Δ be an upper bound on the diameter of area A.

1. **do**

   draw M_o, M_1 $iid\, Unif(A)$

   draw V $Unif[0, \Delta]$

   until $V < \|M_1 - M_0\|$

   $Prev(t) = M_o$ and $Next(t) = M_1$

2. Draw $U \sim Unif[0, 1]$
3. $M = (1 - U)M_0 + UM_1$

M_o and M_1 are initial and next waypoint, respectively. Note that the initial waypoint of time stationary waypoint simulation is obtained by the above procedure, not by drawing a point uniformly in A. Once a node reaches the initial next waypoint, the later next waypoint is chosen uniformly. In our simulation, the mobile velocity is always constant. So, we don't consider time stationary distribution of the mobile speed. There are 15 mobiles in the area of $5Km$ x $5Km$. Mobile speed is constant as $30Km/h$. Warmed-up and final status are at 1,000 and 15,000 time slots of running, respectively. Throughput is counted after warmed-up status. The simulation result is shown in Section 3.5

3.5 Simulation and Results

The performance of simulcasting in ad hoc networks is evaluated using the analytical expressions described previously in this chapter and Monte Carlo simulations. We used a custom simulation programmed in MATLAB because this provided us a simple approach to develop a simulation that incorporates the ability to transmit multiple packets to multiple different receivers in a single transmission slot and to adapt the link- and network-layer protocols to take advantage of the simulcasting capability. We begin by considering the link throughput for the fixed network topology of ten nodes illustrated

Table 3–1. Position of radios in ten-node network in Fig. 2–3

Node ID	X position (km)	Y position (km)
1	1.15	2.00
2	1.53	3.59
3	1.95	2.55
4	3.50	2.25
5	2.40	3.21
6	2.55	2.12
7	3.71	2.57
8	3.10	4.01
9	2.58	4.18
10	2.06	2.00

in Figure 2–3. The positions of these radios are given in Table 3–1. The network degree is 2.2. The link distances are figured out with incorporation of transmission in additive white Gaussian noise (AWGN), where the bit error probability at the maximum transmission range of 1 km is 10^{-4}. It is assumed that the packet length is 1000 bits and an error-control code is used that can correct up to 10 bit errors. For this case of no mobility, we expect that there will be almost no performance degradation from the noise, as the transmission range for nodes to be considered neighbors is such that the packet error probability is very small. The simulation results match closely with the analytical results.

The results in Figure 3–14 show the link throughput performance of the network as a function of the average attempt rate. Solid lines represent the performance predicted by the analysis from (3–2) to (3–5), and (3–7). The markers illustrate the performance results from our simulation. The performance is illustrated for three different network configurations. For the results marked “Unicast”, the nodes are constrained to not employ the simulcast signaling technique, and thus each node transmits at most one packet in a time slot. For the results marked “Simulcast(NW1)”, simulcast transmission is used, where the more-capable links are determined based on a degradation of 0.5 dB and a disparity of 9.1 dB.

The results marked “Simulcast(NW2)” illustrate the performance for a network with fewer more-capable links because the required capability disparity is increased to $11.4dB$, which corresponds to a degradation of 0.3 dB. The link throughput for these fixed topologies with equal back-off times is illustrated in Figure 3–14. The results indicate that simulcasting can significantly improve the throughput in the ad hoc network.

Next, let us consider a network with $N = 15$ radios placed uniformly over a $1km$ by $1km$ area. We consider the simple good/bad channel model with a maximum link distance for unicasting (or, equivalently, simulcasting with $\theta = 0^o$) of 381 m. We consider first some basic network parameters as a function of the offset angle θ of the nonuniform QPSK used for simulcasting. The results in Figure 3–15 illustrate the network degree (expected number of neighbors) as a function of the offset angle θ. The analytical results are determined from (3–1). The simulation results are shown for two cases. The results for “all networks” is the average over 100 random topologies. The results for “connected networks only” shows the average network degree for 10 of the random topologies that formed a connected network for all degrees. The results show the sensitivity of the network degree to the parameter θ. For all networks, unicasting ($\theta = 0$) yields a network degree of approximately 4.5, while for QPSK ($\theta = 45$ degrees), the network degree drops to 3.4. We note that if we consider only connected networks, then the network degree is biased above the value for all networks.

One of the primary effects of changes in the network degree is an impact on the connectivity, which we define as the probability that every node has a route to every other node in a randomly generated network. The connectivity is shown as a function of the offset angle θ in Figure 3–16. The unicast link distance of $381m$ was chosen because it provides connectivity of approximately 0.9. The network connectivity decreases as θ increases. However, for $\theta < 25$ degrees, the connectivity remains above 0.85. Thus, if θ is kept small, simulcasting can be used with relatively little impact on network connectivity. As θ approaches its maximum value of 45 degrees, the connectivity rapidly decreases to

approximately 0.66. Thus, it is not possible to switch to a uniform QPSK constellation without a significant loss in network connectivity.

The results in Figure 3–17 show the expected proportion of radios that have a more-capable link as a function of θ. As shown in Section 3.1, this parameter has an important effect on both the link and end-to-end throughputs. The results show that as θ increases from 0, the proportion of radios with a more-capable link increases rapidly. The analytical expression (3–2) is shown to closely match the simulation results. There is no significant effect on this parameter of only considering connected networks instead of all randomly generated networks. At the previously mentioned value of $\theta = 25$ degrees, the proportion of radios with a more-capable link exceeds 0.8. Thus, there is little to gain from increasing θ further, and any further increase comes at a significant expense in terms of network connectivity, as shown in Figure 3–16.

We next restricted the simulations to 10 fixed topologies that are connected for all $0 \leq \theta \leq 45$ degrees, which were randomly selected from the 100 randomly generated topologies. In this way, we can be sure that we can calculate end-to-end throughput for each network. However, the distribution of the nodes will no longer be uniform, which will affect the results. Each topology still consists of 15 nodes distributed over a 1 km 1 km area, with maximum link distance of 381 m for unicasting. Each simulation consisted of 1500 time slots after a 100 time slot warm-up period.

The results in Figure 3–18 show the average link throughput for unicasting and simulcasting with offset angle $\theta = 25$ degrees for the networks described above. The lines represent analytical results and the markers represent simulation results. The simulation and analytical results differ slightly because the analytical results are for randomly generated networks, but the simulation results are for a set of connected networks. The results show that for $\theta = 25$ degrees, the maximum link throughput is almost twice as high with simulcasting as can be achieved with unicasting. From Figure 3–16, the network connectivity for $\theta = 25$ degrees is approximately 0.85 versus 0.9 for

unicasting, so the link throughput can be significantly increased with little cost to network connectivity.

The results in Figure 3–19 show the maximum link throughput achieved as a function of the offset angle . Here, the maximum is taken over all possible attempt rates. The line is the analytical result, and the circles are from simulations. Note that as θ increases, so does the link throughput that can be achieved. This is reasonable because as long as the network remains connected, each node will have at least one node to which it can transmit. Furthermore, as θ increases, the probability of collision goes down along with the expected number of neighbors, and the number of nodes with more-capable links goes up. The combined effect is that the maximum throughput with $\theta = 45$ degrees is approximately 2.7 times higher than the maximum throughput with unicasting. However, from Figure 3–16, we see that the network connectivity suffers greatly as θ becomes large.

In addition to the impact on network connectivity, increasing θ also affects the length of routes in the network, which may impact the end-to-end throughput. The results in Figure 3–20 illustrate the average number of hops in a route as a function of the offset angle. As θ increases from 0 to 45 degrees, the average number of hops increases from approximately 2.25 to 4.2. The number of hops increases rapidly as θ increases beyond 20 degrees. The results in Figure 3–21 illustrate the maximum average end-to-end throughput as a function of θ. Here, the maximum is over all attempt rates. The solid line illustrates the analytical results (using the empirical values for the expected number of hopes), and the simulation results are the circles. The results show that the end-to-end throughput is a non-monotonic function of θ. The analytical results are optimistic for $\theta > 10$ degrees. However, they do show the same trends as the analytical results. We believe that the primary differences in the two curves come from the fact that the simulation results are not for randomly generated networks because we have enforced that the networks must be connected. The simulation results show

that the end-to-end throughput is maximized by $\theta = 30$ degrees. The end-to-end throughput at $\theta = 30$ degrees is approximately 0.042 versus 0.027 for unicasting. Thus, simulcasting results in an increase in end-to-end throughput of over 55%. If we use a more conservative value of θ in the range $20 \leq \theta \leq 25$, then the end-to-end throughput is still more than 40% higher than unicasting, while having a smaller impact on network connectivity. Note that these values of θ match closely with those found via analysis in Section 3 for a infinite network with a geometric distribution for the number of hops in a route.

We next investigate the effect of having out-of-date information about the network links because of mobility. A radio's link information may indicate that a node is a neighbor even though that a radio has moved out of range. Similarly, a radio may believe that a link is a more-capable link even though the radio's movements have reduced the capability of a link to an extent that the packet error probability over that link degrades performance. We model these effects by only allowing for a periodic update of routing tables. We assume a slot time of $20ms$ and a routing table update every 300 slots (6 s). Fifteen mobiles move around with constant velocities of 30, 50, or 100 km/hr in a $5Km$ x $5Km$ area. We employed the time stationary random waypoint mobility model described above.

Figures 3–22 and 3–23 show the simulation results for the link and the end-to-end throughputs, respectively. They show that the throughputs for both unicasting and simulcasting degrade as velocities increase. However, simulcasting still provides a significant throughput gain. As expected, higher mobility levels generally result in lower throughput as routing table information is more likely incorrect. This is observed to be especially true at high average attempt rates.

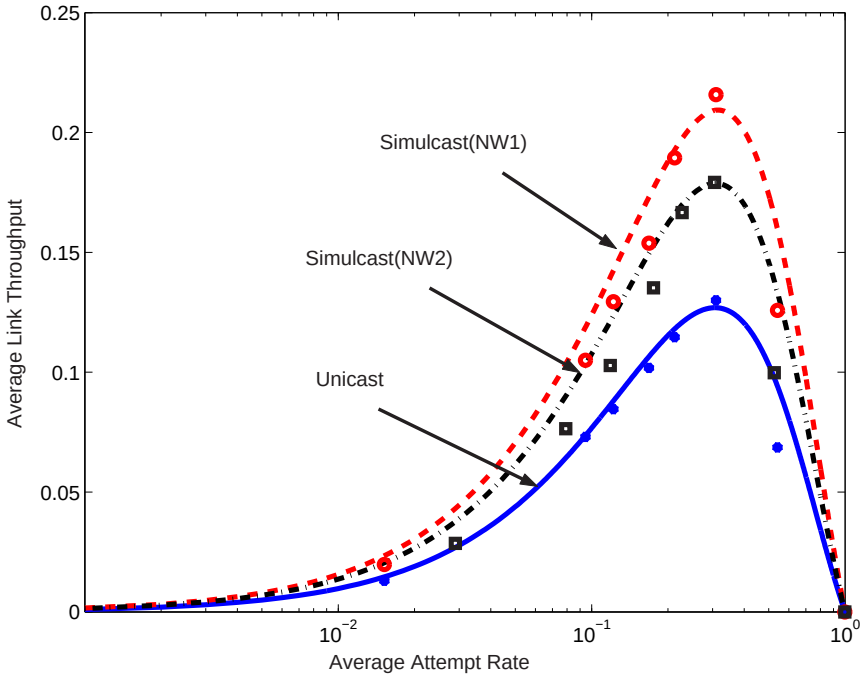

Figure 3–14. Throughput in AWGN for the network of nodes that is illustrated in Fig.3. For NW1, the degradation is 0.5dB, and the disparity is 9.1 dB. For NW2, the degradation is 0.3dB and the disparity is 11.4dB.

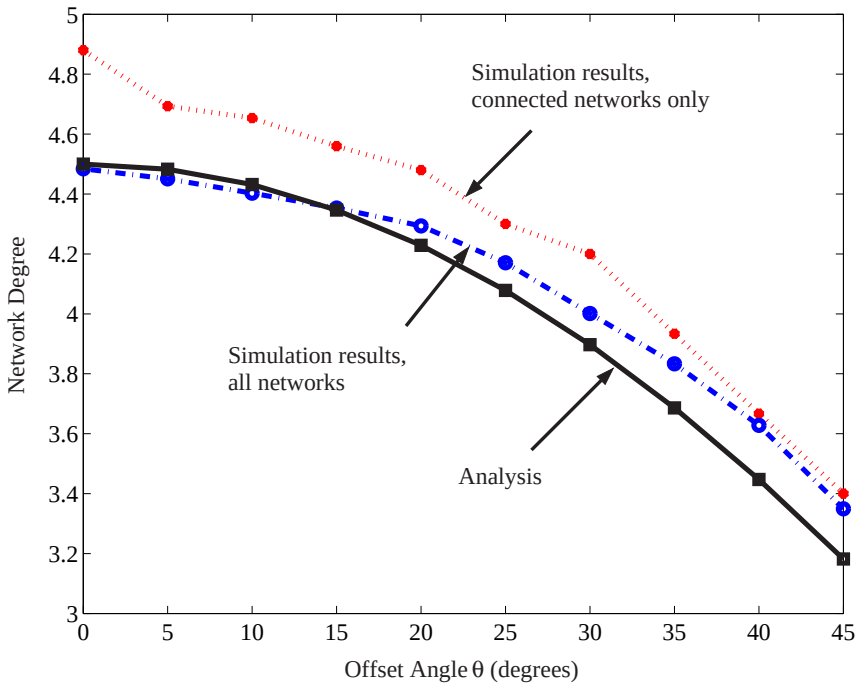

Figure 3–15. Network degree as a function of θ for simulcasting with nonuniform QPSK in a wireless ad hoc network with random node placement.

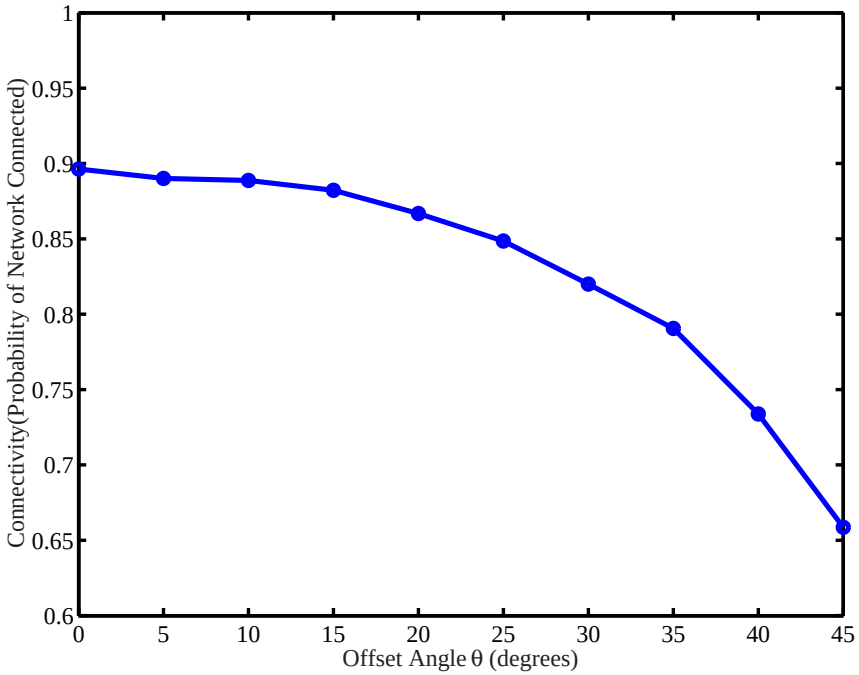

Figure 3–16. Network connectivity as a function of θ for simulcasting with nonuniform QPSK in a wireless ad hoc network with random node placement.

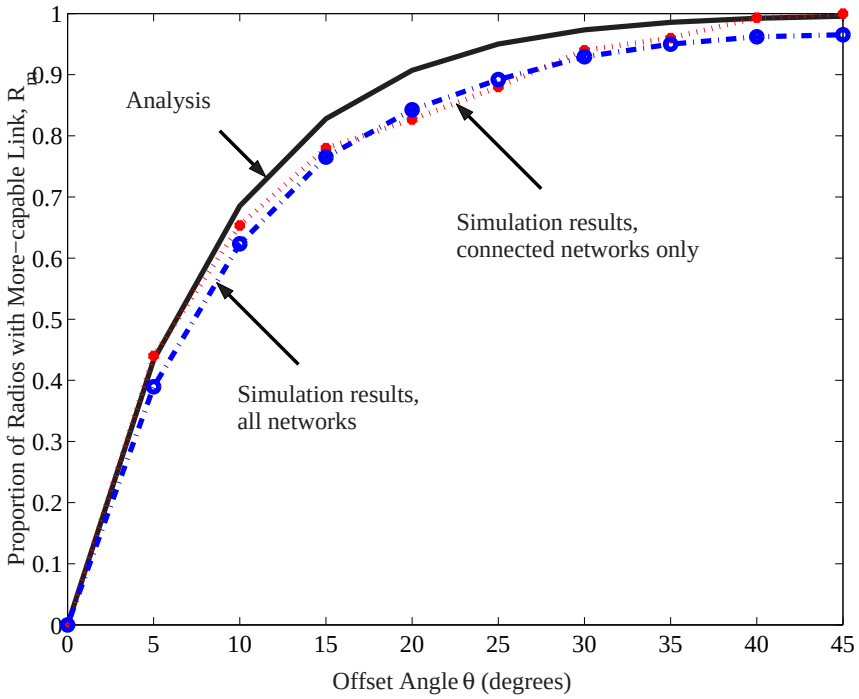

Figure 3–17. Proportion of nodes with a more-capable link as a function of θ for simulcasting with nonuniform QPSK in a wireless ad hoc network with random node placement.

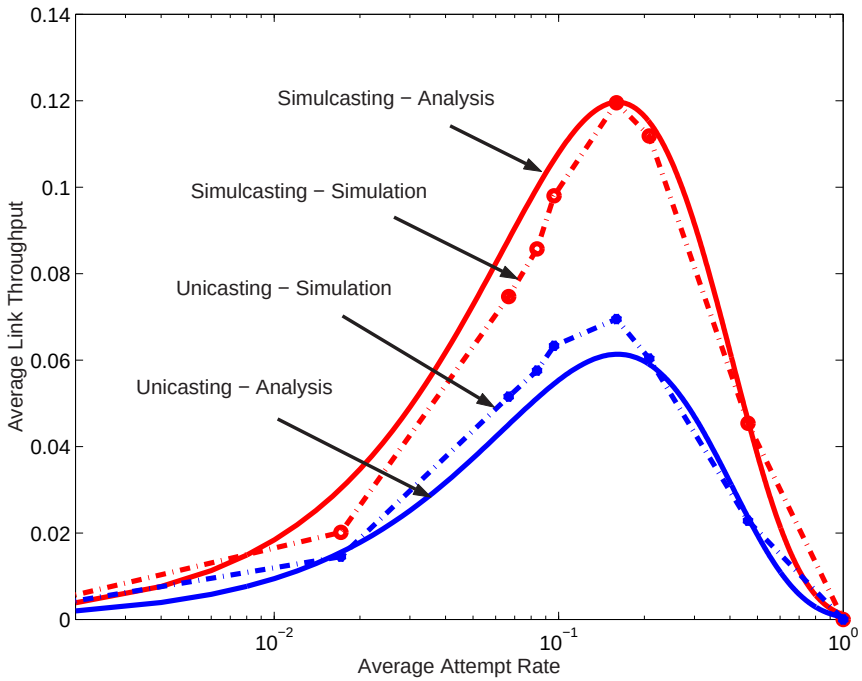

Figure 3–18. Link throughput for unicasting and simulcasting with nonuniform QPSK with $\theta = 25$ degrees in a wireless ad hoc network with random node placement.

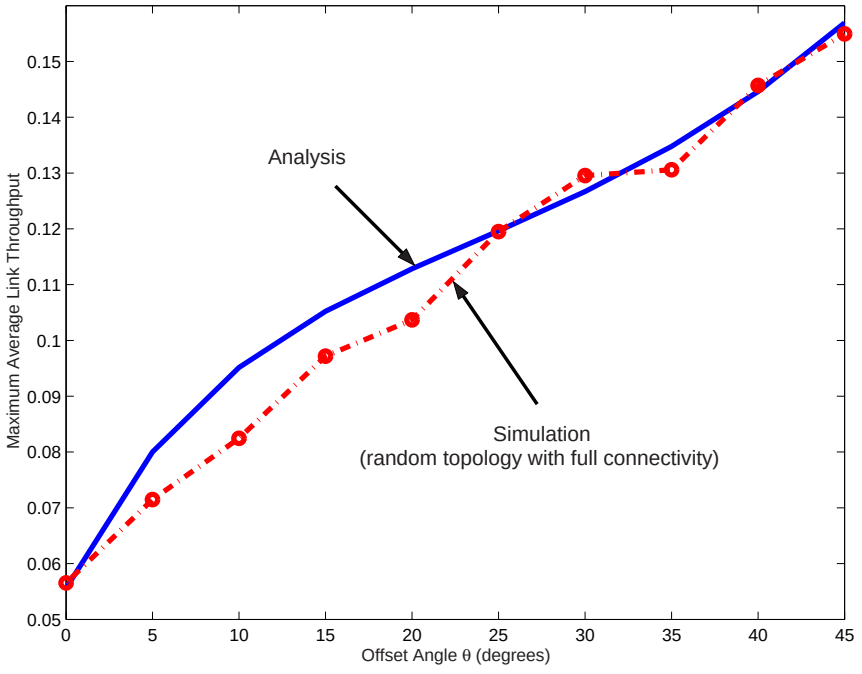

Figure 3–19. Maximum link throughput for simulcasting with nonuniform QPSK as a function of the offset angle θ.

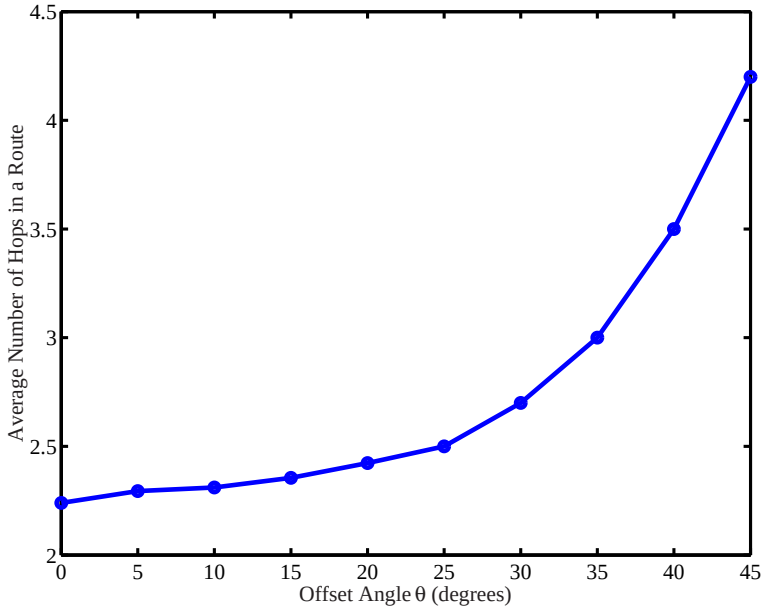

Figure 3–20. Average number of hops in a route for simulcasting with nonuniform QPSK as a function of the offset angle θ.

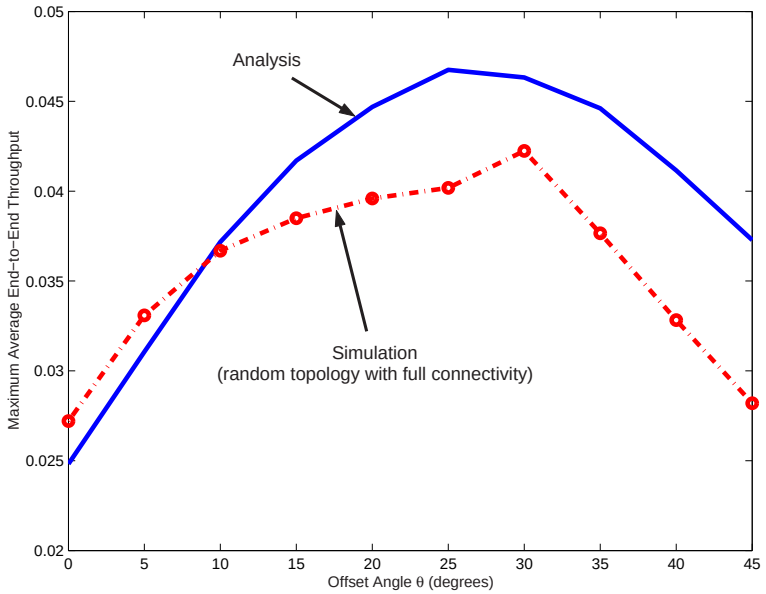

Figure 3–21. Maximum (over all attempt rates) end-to-end throughput for simulcasting with nonuniform QPSK as a function of offset angle θ.

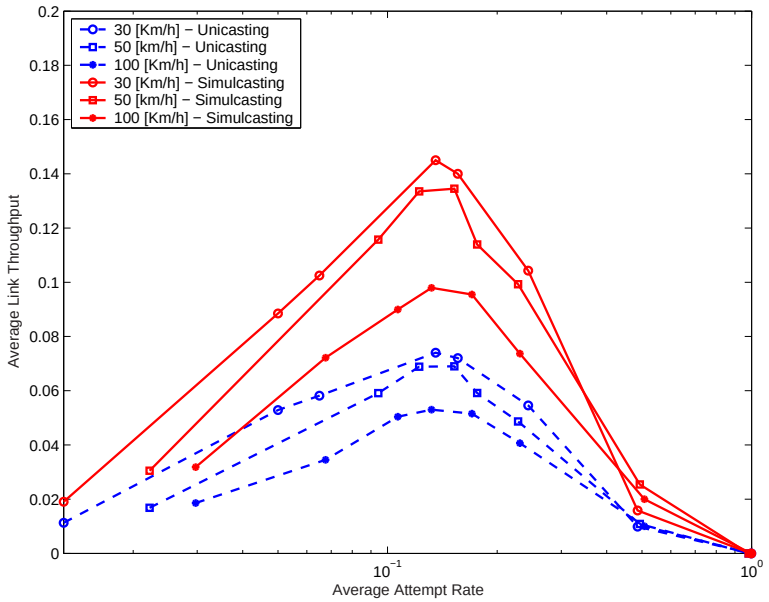

Figure 3–22. Link throughput in AWGN for a mobile network of 15 radios with degradation of 0.5dB and disparity of 9.1 dB by the time stationary random waypoint simulation.

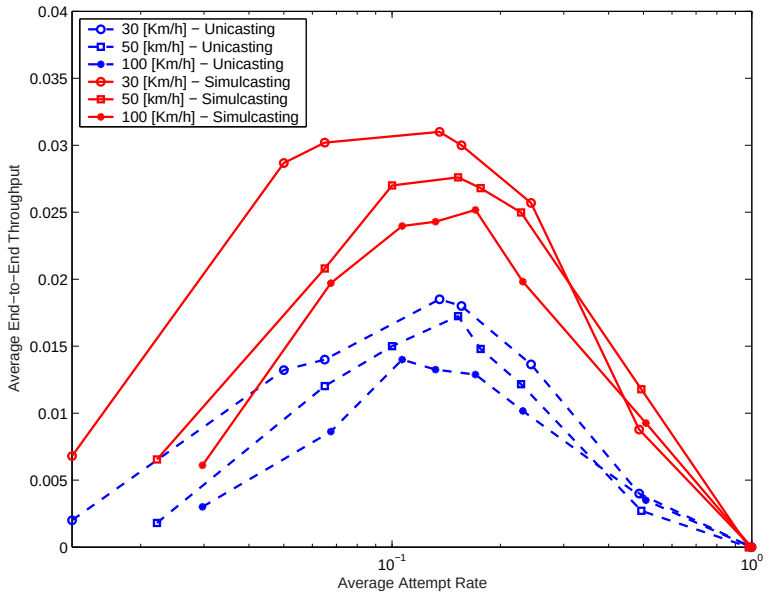

Figure 3–23. End-to-end throughput in AWGN for a mobile network of 15 radios with degradation of 0.5dB and disparity of 9.1 dB by the time stationary random waypoint simulation.

CHAPTER 4
PERFORMANCE OF SIMULCASTING WITH ADAPTIVE BACK-OFF ALGORITHMS FOR SIMULCASTING

When a radio suffers a collision, the radio will wait a random back-off time that is selected according to a geometric distribution. If the average value of the back-off time is specified as T_B, then the radio will begin its retransmission in each of the following slots with probability ${T_B}^{-1}$. So far, our study was based on assigning equal probability of retransmission to every radio when a source radio recognizes that the transmitted packet has collided with another transmission. In this dissertation, we investigate two approaches to choose the parameter T_B. In the first approach, the back-off time is equal for every radio, named as "*Equal Back-off (EQB)*". The performance of simulcasting with this scheme was already investigated in Chapter 3. The radios simulcasting can transmit two packets while the radios unicasting can do just one packet per time slot, which means resource utility available for the radios simulcasting can be up to twice that for the radio unicasting. The second approach, the focus of this chapter, is named as "*Priority Back-off(PRB)*". In *PRB*, the back-off time is chosen unequally to give higher retransmission probabilities to radios simulcasting than to radios unicasting.

We investigate the fairness of each scheme in terms of the achieved throughputs across the radios in the network. The most simple interpretation of the fairness is how close the distribution is to even sharing of resources among all the radios in a network. However, the concept of fairness is multi-faceted depending on its application. For example, as defined in [13], in terms of the equality of each radio's link throughput, fairness should be taken as evenness, defined as "*service fairness*", but in terms of maximization of network throughput, it should be taken as each radio's effective utilization amount, defined as "*effort fairness*". In this dissertation, Dianati *et al.*'s fair share allocation and

utility based fairness [13] are modified to allocate back-off time unequally according to simulcasting capability, and to measure "*service fairness*" and "*effort fairness*" when *PRB* is applied.

4.1 Priority Back-off

In this section, we modified Dianati *et al.*'s fair share allocation scheme [13] to assigns a higher chance of retransmission in each slot to the radios that have more-capable links. The normalized fair share resource allocation of radio i is defined as

$$S_i^{(a)} = \frac{1}{N_t} + \left(S_i^{(u)} - \frac{1}{N_t} \right) \alpha^A, \tag{4–1}$$

where N_t is the total number of radios, α^A is a constant from 0 to 1, and

$$S_i^{(u)} = \frac{[1 + m_i(\theta)]}{\sum_i^{N_t} [1 + m_i(\theta)]}. \tag{4–2}$$

Here, α^A is used to trade off between *service fairness* and *effort fairness*. When $\alpha^A = 0$, $S_i^{(a)}$ is not sensitive to the *effort fairness*, and when $\alpha^A = 1$, $S_i^{(a)}$ has maximum sensitivity to the *effort fairness*. We consider $\alpha^A = 0$, $1/2$, or 1 for our work, where $\alpha^A = 0$ gives equal share amount, $\alpha^A = 1/2$ gives equal sensitivity to sharing the common resource (*service fairness*) to using it efficiently (*effort fairness*), and $\alpha^A = 1$ gives maximized sensitivity to *effort fairness* for resource allocation .Then,

$$S_i^{(a)} = \begin{cases} S_{i,0}^{(a)} = (1 - \alpha^A)\frac{1}{N_t} + \frac{\alpha^A}{N_t[1+R_m(\theta)]}, & m_i(\theta) = 0, \\ S_{i,1}^{(a)} = (1 - \alpha^A)\frac{1}{N_t} + \frac{2\alpha^A}{N_t[1+R_m(\theta)]}, & m_i(\theta) = 1. \end{cases}$$

We select the unequal back-off time $T_{B,j}^P$ for *PRB* with simulcasting based according to

$$T_{B,j}^P = \frac{T_B^E}{K S_i^{(a)}}. \tag{4–3}$$

where, T_B^E is back-off time by *EQB* at a corresponding average attempt rate G, and K is a constant to adjust the resultant back-off time to yield the average attempt rate G by T_B^E.

4.2 Fairness Index

Using unequal back-off parameters can improve link throughput at the expense of evenness. For instance, the parameters can be such that radios simulcasting will nearly always be able to transmit while the other radios are blocked. The link throughput increases because there are few collisions for the radios simulcasting by blocking the radios unicasting, but the network might become useless as the unequal back-off scheme would cause significant blocking of a certain radios unicasting. Therefore, in comparing different back-off parameters, we also consider the fairness provided using two different fairness metrics. The first is the well known "*Min-max index(MMI)*" [14] which compares the ratio of the minimum to the maximum amount of allocated resources among all the users in a network as below, where x_i is the amount of allocated resource to user i. In this dissertation x_i is replaced with the achieved link throughput of radio i.

$$I_{min-max} = \frac{min(x_i)}{max(x_i)}. \tag{4–4}$$

As we discussed fairness has different facets specified differently in the different domain of resource allocation. In other words, fairness cannot always be considered as even resource distribution because a system which is fair in terms of evenness (*service fairness*) may not be fair if it is viewed in terms of the resource allocation amount to each users to maximize network performances (*effort fairness*) when they have different resource utilizing capabilities. Dianati *et al.* proposed in [13] the "*Utility Fairness Index(UFI)*" to capture the fairness sensitive to *effort fairness*. For example, in our simulcasting system, it makes sense to provide additional resources to those radios that

can send at a higher rate (simulcasting), and they should not be penalized for that in the fairness in the view point of optimized resource utilization.

By the application of Dianati *et al.* [13], the normalized achieved throughput is defined as

$$s_i = \frac{x_i}{\sum x_i}. \tag{4–5}$$

The value of x_i is replaced with link throughput of radio i, over a certain attempt rate G. Then, the utility function $U_i(s_i^{(f)})$ with the fair share allocation at a certain value of α is defined as

$$U_i(S_i^{(f)}) = \begin{cases} \sqrt{s_i}, & s_i \leq S_i^{(f)} \\ \sqrt{S_i^{(f)}}, & \text{other wise} \end{cases},$$

where

$$S_i^{(f)} = \frac{1}{N_t} + \left[\frac{1 + m_i(\theta)}{\sum_i (1 + m_i(\theta))} - \frac{1}{N_t}\right] \alpha^F \tag{4–6}$$

is the fair share of radio i, and α^F indicates the trade off between *service fairness* and *effort fairness*. Then, the "*Utility Fairness Index(UFI)*", is defined as in [13] as

$$F(x) = \left[\frac{\sum_{i=1}^{n} U_i(S_i^{(f)})}{\sum_{i=1}^{n} \sqrt{S_i^{(f)}}}\right]^2. \tag{4–7}$$

4.3 Simulation and Results

We perform simulation of back-off allocation by PRB based on utility based back-off allocation in the random network previously described in Section 3.5. Simulations are carried out with various values of α^A. The markers $*$, $\circ$, and $\square$ represent the results for α^A is equal to 0.0, 0.5, and 1.0, respectively. The 100 different uniformly distributed random networks have been generated, and 4 fully connected networks are chosen for

simulation among them. The running time is 5,000 time slots for each random network. The simulation results are averaged over the 4 fully connected networks.

The results in Figure 4–1 shows the simulation results of maximum link throughput as a function of the offset angle θ. The maximum is taken over all possible attempt rates as in Section 3.5. Note that as θ increases, so does the link throughput that can be achieved. The results show that, in the relatively large range of offset angle, from 15 to 40 degree, the maximum link throughput increases up to about 10% and 20% by PRB with α^A equal to 0.5 and 1.0, respectively.

The results in Figure 4–2 shows the simulation results of maximum end-to-end throughput as a function of θ. The maximum is taken over all possible attempt rates as we discussed. The results show that the end-to-end throughput is a non-monotonic function of θ. The simulation results show that the end-to-end throughput is maximized by $\theta = 20$ degrees. The results show that, in the relatively large range of offset angle, from 15 to 40 degree, the maximum end-to-end throughput also increase up to about from 3% to 10% by PRB with α^A equal to 0.5 and 1.0, respectively.

Figure 4–3 shows the simulation results of *MMI* as a function of θ. The results show that the *evenness* degrades as we allocate back-off to be more sensitive to *effort fairness*. The evenness for all three cases with different α^A values decline when θ is over 25 degrees.

Figure 4–4 shows the simulation results of *UFI* as a function of θ. The *UFI* is observed at the same values of α^F with α^A of fair share resource allocation except for the marker $\triangle$ which indicates the case with $\alpha^A = 1.0$, fully sensitive to *effort fairness* for the fair share resource allocation, and $\alpha^F = 0.0$, fully sensitive to *service fairness* for the fairness index. The results show that while the *service fairness* is degraded by *PRB*, there's no big change in *UFI* as the value of α^A increases compared to *MMI*. However, the *UFI* also become worse as α^A increases, which means, as same reason with *MMI*

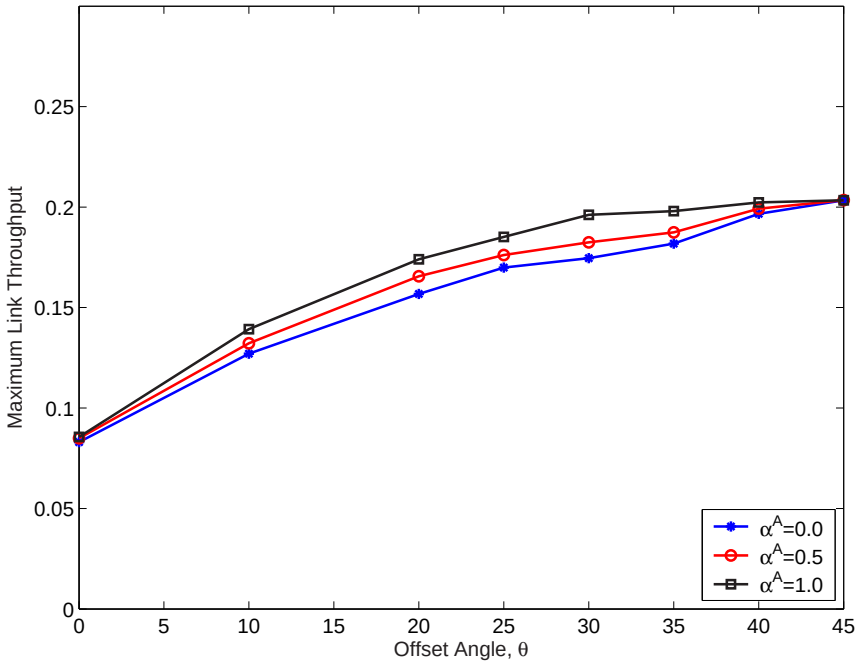

Figure 4–1. Maximum link throughput by PRB with various α^A values in random network topology as the function of offset angle θ.

case, *PRB* is dependent of R_m, and becomes more sensitive at the value of θ over 25 degrees.

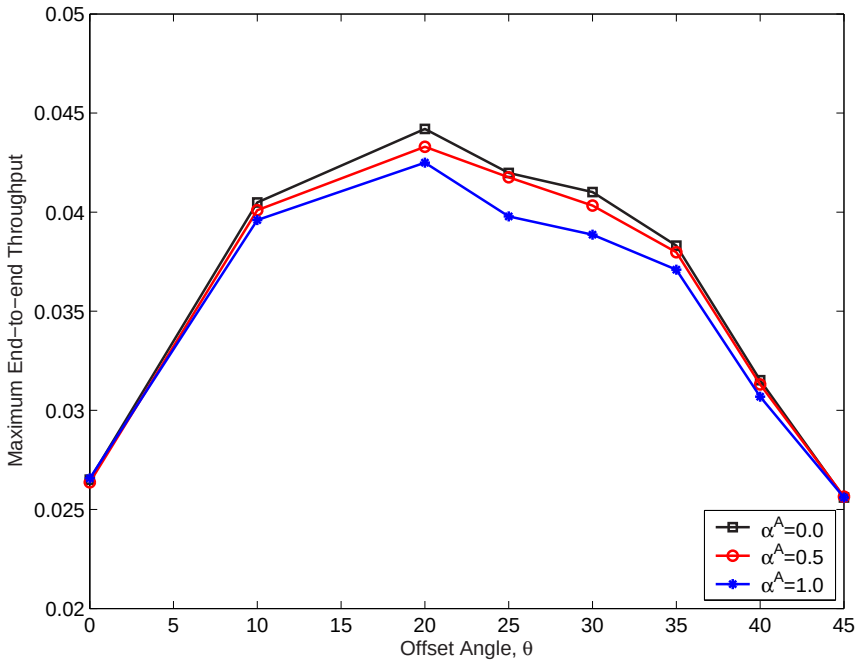

Figure 4–2. Maximum end-to-end throughput by PRB with various α^A values in random network topology as the function of offset angle θ.

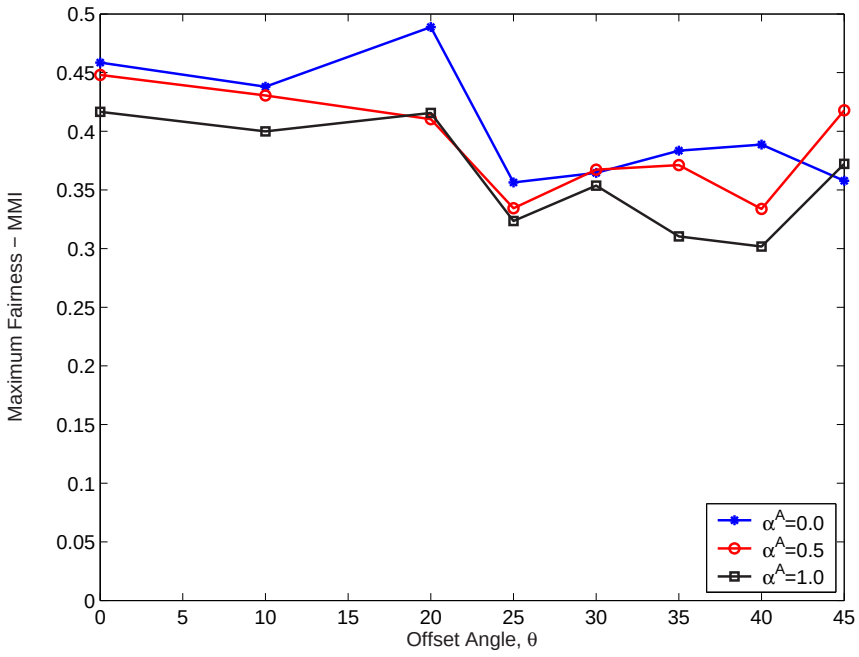

Figure 4–3. Min-max fairness by PRB with various α^A values in random network topology as the function of offset angle θ.

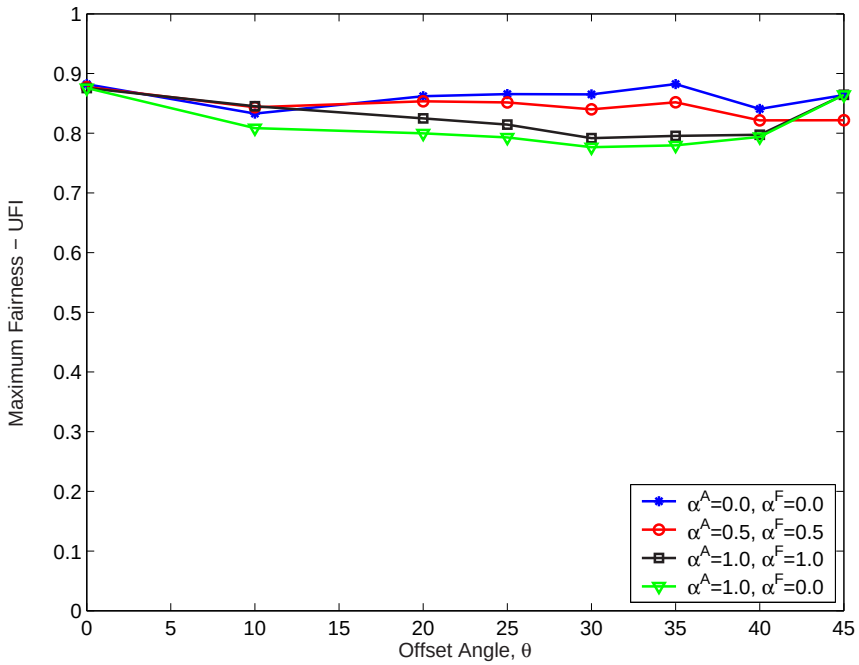

Figure 4–4. Utility based fairness by PRB with various α^F and α^A values in random network topology as the function of offset angle θ.

CHAPTER 5
UNEQUAL RANDOM ROUTE SELECTION FOR SIMULCASTING

In this chapter, we investigate how the simulcasting capability can be exploited at the network layer by adjusting the distribution of packets across multiple routes in a system employing multipath routing. The modified min-hop routing for simulcasting that we use in previous sections in this dissertation is presented in Section 2.3. Based on this min-hop routing algorithm, we may have several routes that have same number of hops from a source radio to a final destination. However, each route is still likely to differ in terms of simulcasting capability because of different numbers of relay radios with more-capable links. Routes that have more relay radios with more-capable links will transmit more packets per transmission opportunity and therefore be more efficient in relaying a packet along the route. If a radio has multiple routes to a destination, this effect should be considered when determining what proportion of packets to transmit on a route. In this chapter, we provide a preliminary investigation of how simulcasting capability can be exploited in the network layer in the allocation of packets across multiple routes. We investigate the performance of varying the packet distribution across routes with different simulcasting capabilities for several network topologies.

5.1 Network Model

The example networks that we consider have a source(S) and a destination(D) radio connected by two routes with same number of hops but different simulcasting capabilities. The three network topologies that we consider are shown in Figures 5–2–5–4. In order to reduce the simulation complexity and run time, we do not simulate radios in the network other than those on the two routes from S to D as if they were part of a larger network. Every radio is modeled as having the same average attempt rate G and same number of neighbors N_b, which is defined as the network degree. So, given a

transmission, the collision probability is $P_C = \sum_{i=1}^{N_b} C_i^{N_b} G^i (1-G)^{N_b - i}$ as in Section 3.2.1. Then the link throughput by unicasting is given by $S_U = G(1-P_C)$ and by simulcasting is $S_S \approx 2G(1-P_C)$, as in Chapter 2. These values determine statistics of the queue, such as the arrival and the service rates for a queue of a relay radio on a route. If a packet from the source radio collides with another transmission at one of the radios along the route, the packet will stay in the queue of the transmitting radio to wait for re-transmission.

We consider a multipath routing scheme in which packets from S are distributed across the two routes according to a random distribution,as illustrated in Figure 5–1. The source S transmits packets at attempt rate G to only the destination D. The two routes have same number of hops to D, but may have different simulcasting capabilities. We define the *more-capable route* as the route which has larger simulcasting capability, and the *less-capable route* as the route which has less simulcasting capability. We select a route for transmission randomly with probability $R1$ for the *more-capable route* and $R2$ for the *less-capable route* at each transmission, where $R1 + R2 = 1$. We also define the *optimal route selection rate* as the route selection rate for the *more-capable route* to achieve the maximum end-to-end throughput.

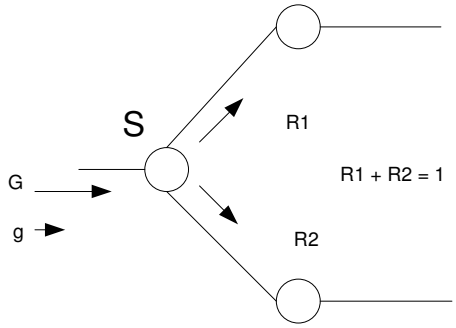

Figure 5–1. Packet transmission from source radio to randomly selected route based on simulcasting capability.

We model three topologies of transmission routes in wireless ad hoc networks with identical wireless radios deployed within a two-dimensional geographical territory. There are two routes as we mentioned above. The two routes have same number of hops from source radio to destination radio, but different simulcasting capabilities due to the number of relay radios with simulcasting, or different number of more capable links along each route. The upper route is the *more-capable route*, and the lower route is the *less-capable route*. We assume that each route does not interfere with each other because they are not within transmission range. We measure the end-to-end throughput as the number of packets successfully transmitted from S to D per time slot. Figures 5–2–5–4 show the three topologies for which we present results. The filled circles represent radios that can utilize simulcasting because they have more-capable neighbors, and the empty circles represent radios that can only unicast. The bold lines represent more-capable links, and the thin lines represent less-capable links. Topology 2 has more relay radios with simulcasting on the *more-capable route* than on the route of topology 1, but the number of more-capable links are the same. Topology 3 has the same number of relay radios with simulcasting on the *more-capable route* as topology 2, but has more more-capable links. The conditions of the *less-capable route*s are same for all topologies.

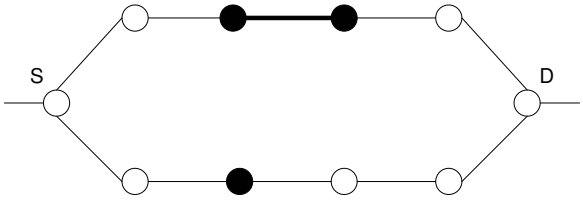

Figure 5–2. Topology 1 for unequal random route selection based on simulcasting capability.

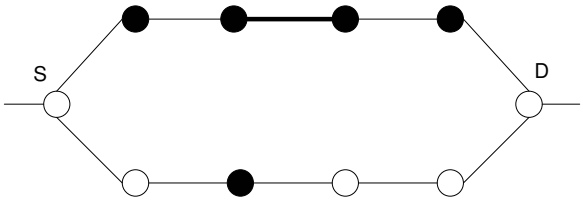

Figure 5–3. Topology 2 for unequal random route selection based on simulcasting capability.

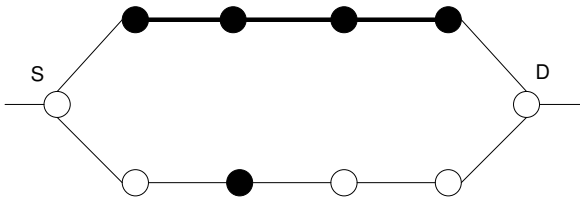

Figure 5–4. Topology 3 for unequal random route selection based on simulcasting capability.

5.2 Link Properties

In this section, we describe how we generate packets at the intermediate radios along the routes from S and D as if these radios were part of a larger network but without simulcasting the other radios in the network. We model the inflow and out flow of traffic to the queue of a radio along the route, as illustrated in Figures 5–5. The states n and $n+1$ in the circles represent the number of packets in the queue, p and q are arrival rate and service rate, respectively. For the purposes of modeling packet arrivals and departures at the radios along the two routes, we treat the arrivals and departures as independent. In fact, these are not independent, as a radio may not successfully transmit and successfully receive simultaneously. However, we expect this approximation will have little impact on our results. Then, Q is the probability of no change in the number of packets after one transmission time slot, which we approximate by $Q = pq + (1-q)(1-p) + (1-p)P(0)$, where $P(0)$ represents the probability that there is no packet in the queue at the current transmission time slot.

The statistics of the queue status depend on the simulcasting capability, which is determined by several network parameters such as the number of neighbors, the number

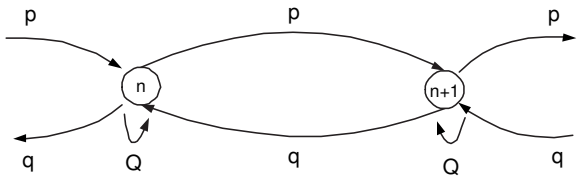

Figure 5–5. Markov status diagram for the number of packets in a queue.

of more-capable links of a radio, and the number of more-capable link on the route. Figures 5–6 – 5–10 illustrate possible link statuses and their properties. The service rate q simply includes any packet outgoing which include the packet from S to D. However, the arrival rate p_b includes only basic message incoming by unicasting, and the arrival rate due to additional messages incoming by simulcasting is represented by the symbol p_a. The traffic generated according to probabilities p_b and p_a is not used to model the traffic from S to D, which is fully simulated. The total incoming rate p is equal to $p_b + p_a$. The dotted arrows in Figures 5–9 and 5–10 represent additional message other than from the source that is received by simulcasting at a radio along the *more-capable route*.

Figure 5–6 represents one of the possible link conditions, *link model 1*, that the relay radio doesn't have any more-capable link. So, it's arrival and service rate correspond to the link throughput by unicasting. However, because the total arrival rate p doesn't include the traffic incoming from S, based on the assumption that every radio involved in the transmission in the network is identical, and send packets uniformly on each branch, the arrival rate p is related with the amount of packets incoming except from one branch among all N_b branches. Then,

$$\begin{aligned} p &= \frac{N_b - 1}{N_b} S_U + g, \\ q &= S_U. \end{aligned}$$

Also, because the link on the route from S is a less-capable link, traffic from the source will be one packet at a time.

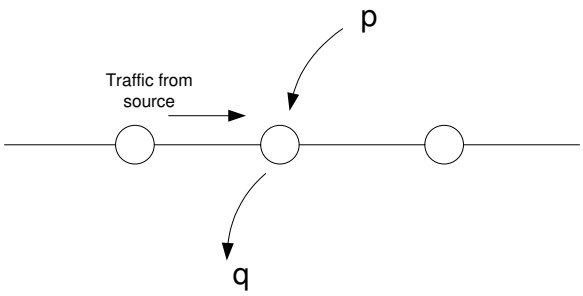

Figure 5–6. *Link model* 1 for analyzing queue status in random route selection based on simulcasting capability. The relay radio doesn't have a more capable link.

Figure 5–7 illustrates another possible link condition, *link model 2*, that the relay radio can simulcast but doesn't have any more-capable link on the route. So, it's arrival and service rate correspond to the link throughput by simulcasitng. The service rate q is simply $2S_U$. The arrival rate p is figured out in similar way with *link model 1*, but corresponds to throughput by simulcasting, and because this relay radio can simulcast, it includes arrival rate for additional message p_a. The relay radio doesn't have any more-capable link on the route, so based on the assumption that sending additional message on each more-capable links is uniform and independent on transmission of basic message, p_a is $S_u(N_m/N_b^2)$. Then, with similar analysis of *link model 1*, where N_m is average number of more-capable links of a radio,

$$\begin{aligned} p &= S_U\left(\frac{N_b-1}{N_b}+\frac{N_m}{N_b^2}\right)+g, \\ q &= 2S_U. \end{aligned}$$

Because the link on the source side on the route is a less-capable link, the traffic coming from that direction arrive one packet per transmission.

Figure 5–8 illustrates another possible link condition, *link model 3* where the relay radio can simulcast and has a more-capable link on the source side on the route. So, it's arrival and service rate correspond to the link throughput by simulcasitng. The service rate q is simply $2S_U$. The arrival rate p is figured out as similar way with *link*

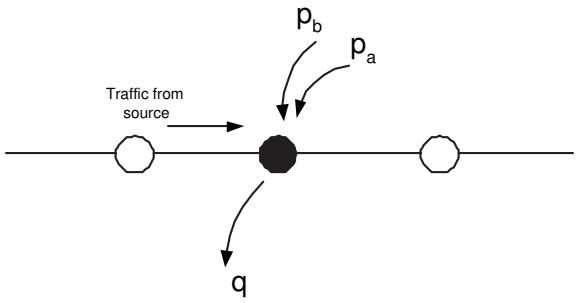

Figure 5–7. *Link model 2* for analyzing queue status in random route selection based on simulcasting capability. The relay radio has more capable links, but not on the route.

model 2. However, one additional message comes from the source side. So, the amount of additional messages included in p_a is lessened by the proportion of one branch among N_m branches. Then, the arrival rate for the additional message is given by $S_U(N_m - 1)/(N_b^2)$. Then,

$$\begin{aligned} p &= S_U \left(\frac{N_b - 1}{N_b} + \frac{N_m - 1}{N_b^2} \right) + g, \\ q &= 2S_U. \end{aligned}$$

Because the link on the source side on the route is a more-capable link, traffic coming from that direction arrive two packets per transmission.

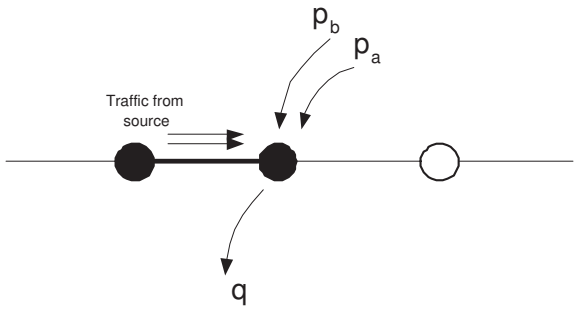

Figure 5–8. *Link model 3* for analyzing queue status in random route selection based on simulcasting capability. The relay radio has more capable links, and one of them is included on the source side of the route.

Figure 5–9 illustrates another possible link condition, *link model 4*, where the relay can simulcast and has more-capable link on the destination side of the route. The only

difference with *link model 3* is that an additional message incoming to the radio is from the destination side. So, the arrival rate for additional message p_a includes the additional message from a radio on the destination side of the route. Then,

$$\begin{aligned} p &= S_U(\frac{N_b - 1}{N_b} + \frac{N_m}{N_b^2}) + g, \\ q &= 2S_U. \end{aligned}$$

Because the link on the source side of the route is a less-capable link, traffic from the source side will arrive with only one packet per transmission.

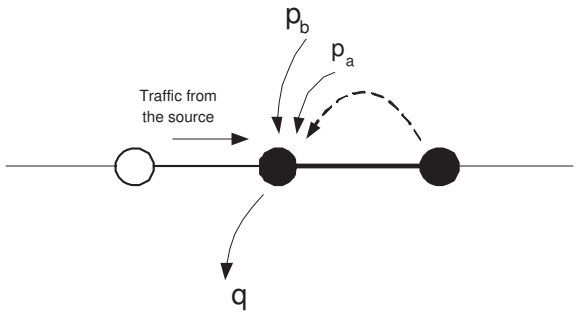

Figure 5–9. *Link model 4* for analyzing queue status in random route selection based on simulcasting capability. The relay radio has more capable links, and one of them is included on the destination side of the route.

Figure 5–10 represents the final possible link condition, *link model 5*, where the relay radio can simulcast and has more-capable links to both neighbors on the route. The arrival rate for additional message p_a in this condition is same with *link model 3*. Then,

$$\begin{aligned} p &= S_U(\frac{N_b - 1}{N_b} + \frac{N_m - 1}{N_b^2}) + g, \\ q &= 2S_U \end{aligned}$$

Because the link on the source side of the route is a more-capable link, the traffic from that direction will arrive with two packets per transmission.

In the above network model, we consider the end-to-end throughput which is measured as the number of packets successfully transmitted from the source radio to the destination radio per time slot. The statistics of the queue delay at each relay radio for the

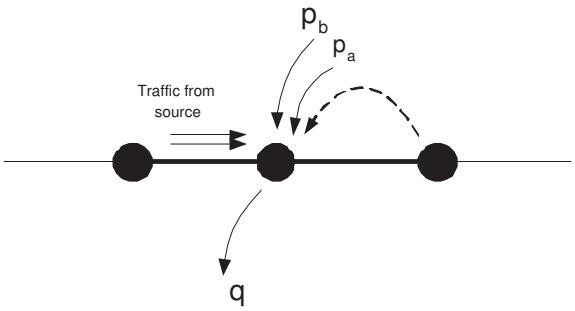

Figure 5–10. *Link model 5* for analyzing queue status in random route selection based on simulcasting capability. The relay radio has more capable links, and two of them are included at the both of source and destination sides of the route.

traffic from the source radio will affect to the end-to-end throughput. Now, we investigate unequal random route selection which randomly assigns an unequal amount of traffic from the source radio to each route.

5.3 Simulation and Results

We performed separate simulations for each of the three network topologies with variations in the network degree and average number of more-capable links of a radio with simulcasting. The source radio transmits packets at the same attempt rate as the rest of the radio in the network, and all the packets transmitted by the source radio are destined to destination radio. We randomly select a route for a packet to be transmitted with probability of $R1$ for the *more-capable route* and $R2$ for the *less-capable route*. The probabilities $R1$ and $R2$ are varied subject to $0 \leq R_1 \leq 1$, $0 \leq R_2 \leq 1$, and $R1 + R2 = 1$. The queue status of each relay radio is determined by the statistics mentioned in Section 5.2. If a packet transmitted from source radio is collided by the collision probability P_C in Section 5.1 at any relay radio on a route, the packet stays in the queue of the original radio to wait for retransmission at average attempt rate G. Simulation is performed on various attempt rates G in the range from 0 to 1. If a packet is successfully transmitted, it moves to the end of the arrival queue of the next radio. The packet selection is based on FIFO as mentioned in Section 2.4. We ran 100,000 time

slots to count the numbers of packets that were transmitted from the source radio and that arrived at destination radio successfully for various probabilities of $R1$ and $R2$.

We also performed simulations for a high-density network scenario in which the network degree is 8 and the average number of more-capable links of a radio with simulcasting is 4, and for a low-density network scenario in which the network degree is 6 and the average number of more-capable links of a radio with simulcasting is 3. The results in Figures 5–11 and 5–12 show the simulation results for maximum throughput in the high-density network and the low-density network, respectively, in each of the three topologies. The marks $*$, $\square$, and $\circ$ represent the simulation results for topology 1, topology 2, and topology 3, respectively. The low-density network results show the same pattern of end-to-end throughput as in the high-density network, but give 43.24%, 32.14%, and 26.79% higher maximum end-to-end throughputs in topology 1, 2, and 3, respectively. We believe that this is because the low number of neighbors gives a lower collision probability at receivers. The results for the high-density network in Figure 5–11 show that topology 2 and 3 give around 52% higher maximum end-to-end throughput than topology 1, but almost no difference between topology 2 and 3. The results for the low-density network in Figure 5–12 show that topology 2 and 3 give 39.62% and 33.96% higher maximum end-to-end throughput than topology 1, respectively, and the difference between topology 2 and 3 is as small as 4.23%. This indicates that the end-to-end throughput using random route selection is strongly dependent on the number of relay radios with simulcasting, but not as much on the number of more-capable links on a route.

The results for the high-density network in Figure 5–11 show that the maximum end-to-end throughputs are improved by 270%, 450%, and 410% for topology 1, 2, and 3, respectively, by random route selection compared to the case that we choose the *less-capable route* only. Compare to the case that we choose the *more-capable route* only, the maximum end-to-end throughput is improved 37.04%, 27.27%, and 33.33%, for topology

1, 2, and 3, respectively, by random route selection. The *optimal route selection rate* is in the range from 0.6 to 0.9 which is over the equal distribution point (0.5) for the topology 2 and 3. For topology 1, it is in the range of 0.3 to 0.9, although it is very slightly higher between 0.7 and 0.9.

The results for the low-density network in Figure 5–12 show that the maximum end-to-end throughputs are improved by 270%, 410% and 390% for topology 1, 2, and 3, respectively, by random route selection compared to the case that we choose the *less-capable route* only. Compare to the case that we choose the *more-capable route* only, maximum end-to-end throughput is improved by 33.3%, 24.1%, and 21.1%, for topology 1, 2, and 3, respectively, by using random route selection. The optimal route selection rate is around 0.5, and 0.7 for topology 1, and topologies 2 and 3, respectively.

The simulation results for both the high-density and low-density network show that the optimal route selection rate is higher for topology 2 and 3 than in topology 1. This indicates that the optimal route selection rate is strongly dependent on the number of relay radios simulcasting on a route. The simulation results indicate that knowledge of the simulcasting capabilities of radios along a route can be utilized in the network layer to improve end-to-end throughput in a system employing multi-path routing.

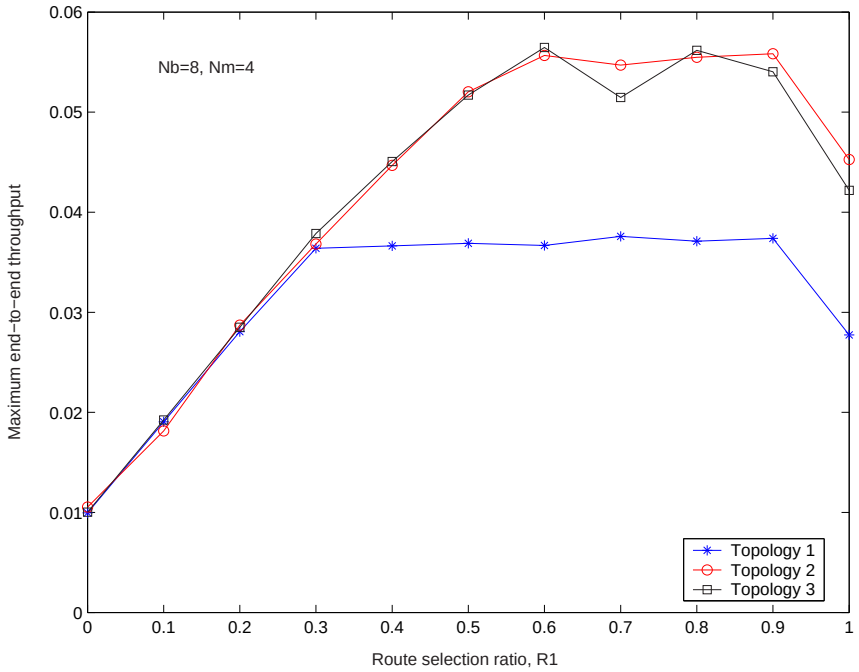

Figure 5–11. Maximum end-to-end throughput versus route selection ration for route 1 at high density network.

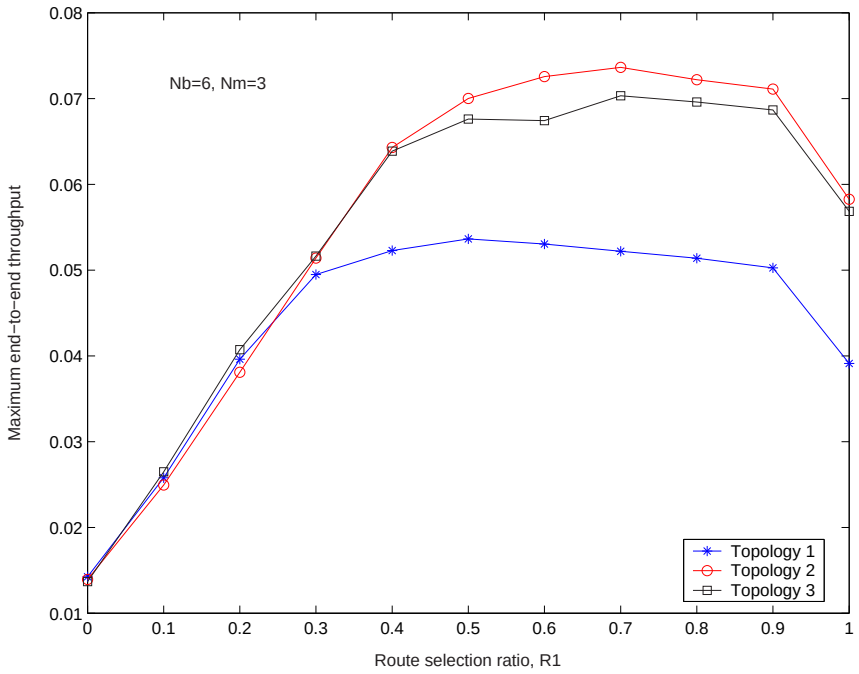

Figure 5–12. Maximum end-to-end throughput versus route selection ration for route 1 at low density network.

CHAPTER 6
UNEQUAL POWER ALLOCATION FOR SIMULCASTING

In this chapter, we show that simulcasting is an effective technique to improve throughput efficiency, which is measured as the throughput per unit energy, and propose some distributed power control approaches to further improve the throughput efficiency of simulcasting. The adaptation of the transmission power and spacing of points in the constellation are considered in order to improve throughput efficiency. In the power control scheme that we consider, the transmission power is adapted based on the link distance of the intended receiver. We also consider the allocation of higher transmission powers for radios simulcasting. Simulation results show that the proposed approaches improve both throughput and throughput efficiency.

6.1 Power Allocation Scheme

6.1.1 Link Adaptive Transmission Power

The proposed strategy in this section is based on the assumption that the transmitter can estimate the signal attenuation at a receiver by a certain channel measurement before the actual transmission. Before the transmitter transmits a packet, it estimates the received transmission power to satisfy target error probabilities for the basic and additional messages, which adaptively determine the signal constellation point for simulcasting. So, the offset angle θ is varied for each transmission based on the condition of the links to the less-capable and more-capable receivers. The main purpose of this scheme is to reduce the transmission power needed while satisfying a certain target error probability, so as to reduce network interference to the rest of the radios in the network and minimize the required transmit energy. The throughput may not be affected with this scheme because the received signal power comes less at the same ratio that the network interference does. However, it is expected to improve network performance in terms of throughput

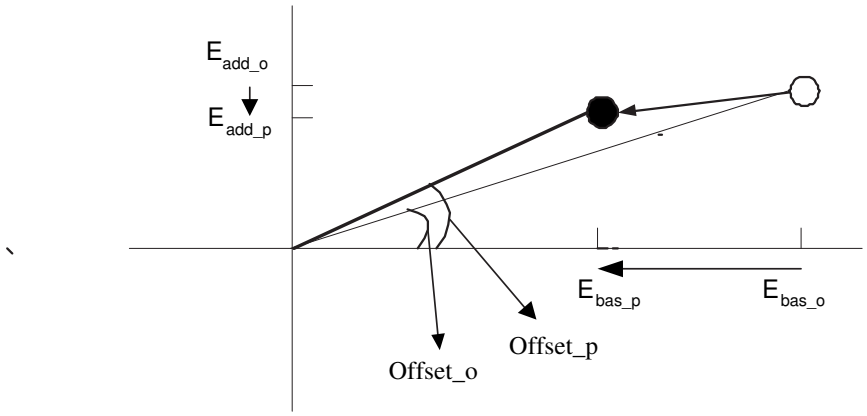

Figure 6–1. Symbol movement by minimized transmission power.

efficiency, which is defined as the throughput per unit energy [60]. Figure 6–1 illustrates the signal constellation change by link adaptive transmission power for simulcasting. $E_{bas,o}$, $E_{add,o}$, and *Offset_o* represent the original, before power control, energy for the basic message, energy for the additional message, and offset angle, respectively. $E_{bas,p}$, $E_{add,p}$, and *Offset_p* represent the power-controlled energy for the basic message, energy for the additional message, and offset angle, respectively.

6.1.2 Unequal Transmission Power Allocation

In order to better utilize the simulcasting capability, we also investigate allocating more transmission power for simulcasting. Because a simulcast transmission delivers two messages at a time, letting simulcasting have a relatively higher probability of successful packet transmission by allocating more transmission energy is expected to increase both throughput and throughput efficiency. In this dissertation, the additional transmission power that is allocated to the radios is a parameter that is varied. Because allocating higher transmission power to the radios simulcasting will cause higher interference to the radios unicasting, the improved network performance by unequal transmission power is achieved at the expense of unbalanced evenness such that the radios simulcasting blocks the radio unicasting. However, as we discussed in Chapter 4, fairness should be interpreted in multi-faceted way. So, in this Chapter, we investigate the fairness described in Chapter 4 when unequal transmission power is applied.

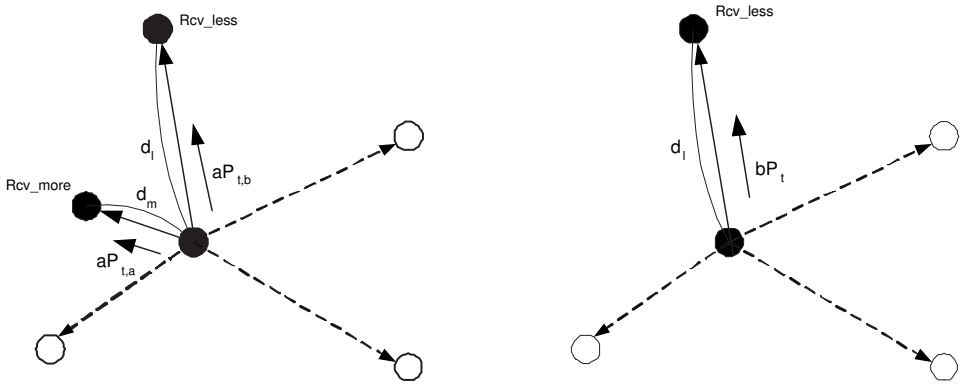

Figure 6–2. Unequal transmission power allocation.

Figure 6–2 illustrates the unequal transmission power allocation scheme. In the figure, d_l and d_m indicate the link distances from the transmitter to the less-capable and more-capable receivers, respectively. P_t indicates transmission power for unicasting, and $P_{t,b}$ and $P_{t,a}$ indicate the transmission power for basic message and additional message, respectively, when a radio is simulcasting. Here α and β, $\alpha \geq \beta$, are power control factor for simulcasting and unicasting, respectively.

6.2 Network Model

Figures 6–3 and 6–4 illustrate the transmission power allocation for unicasting and simulcasting, respectively. We consider only the path loss in computing minimum transmission power P_t, $P_{t,b}$, or $P_{t,a}$ to achieve a target error probability at a receiver in an AWGN channel without consideration of interference. Then the computed minimum transmission power is unequally adjusted by power weights β and α for unicasting and simulcasting, respectively. The weighted transmission power P_U and P_S for unicasting and simulcasting, respectively, are constrained such that the transmission range by power control will not be over the original transmission power range R, which for discussion purpose we normalize to 1.0. We also normalize the original transmission power P_o, which is required for a target error probability at the boundary R, as 1.0. In Figure 6–3, R_M is the transmission range for an additional message, so the radio unicasting exists in the range between R_M and R. R_U is the limit that the transmission range weighted by β

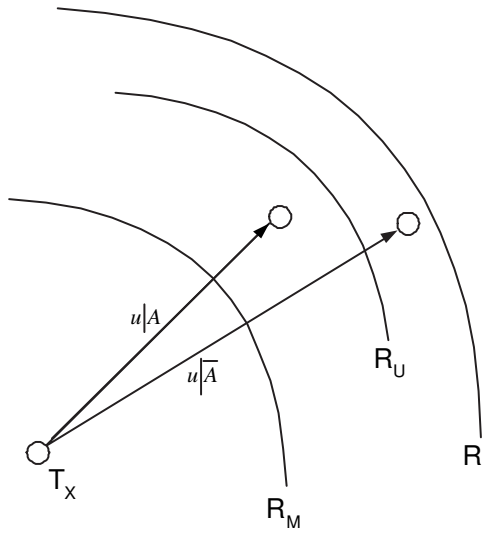

Figure 6–3. Diagram of transmission power range for unicasting.

is not over R when a radio is inside of the range. So, when a radio is outside of R_U, the value of β should be adjusted so as final transmission range is not over R. In Figure 6–4, R_S is the transmission range for basic message and is the limit that the transmission range weighted by α is not over R when a radio is inside of the range. So, when a radio is outside of R_S, the value of α should be adjusted so as final transmission range is not over R.

Let A be the event that a receiver radio is in the range between R_M and R_U, and $\overline{A}$ is the event that the radio is out of R_U. Then the adjusted transmission power for unicasting, P_U, for a certain target error probability at a receiver distance d_l from the transmitter is

$$P_U = \begin{cases} \beta\Delta_U = \beta d_l^n, & A : R_M < d_l \leq R_U \\ 1, & \overline{A} : R_U < d_l \leq 1, \end{cases}$$

where $\Delta_U = d_l^n$. $R_M = 2^{-1/n}$ is the maximum transmission range for additional messages. Similarly, for simulcasting, the adjusted transmission power, P_S, weighted by

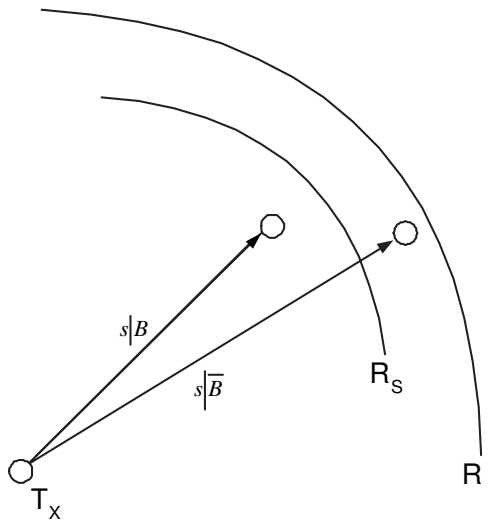

Figure 6–4. Diagram of transmission power range for simulcasting.

the power weight factor for simulcasting, α, is

$$P_S = \begin{cases} \alpha\Delta_S = \alpha\sqrt{d_l^{2n} + d_m^{2n}}, & B : s \le R_S \\ 1, & \overline{B} : s > R_S, \end{cases}$$

where $s = \sqrt{d_l^2 + d_m^2}$ and d_m is the link distance of more-capable receiver. B is the event that a receiver radio is in the range R_S, and $\overline{B}$ is the event that the radio is out of R_S. Then, the received signal strengths $S_{r,U}$ and $S_{r,S}$ by unicasting and simulcasting, respectively, at the receiver sites distances d_l and d_m for the basic and additional message, respectively, are

$$S_{r,U} = \begin{cases} \beta, & A : R_M < u \le R_U \\ d_l^{-n}, & \overline{A} : R_U < u \le 1, \end{cases}$$

$$S_{r,S} = \begin{cases} \alpha, & B : s \le R_S \\ \hat{s}^{-n}, & \overline{B} : s > R_S, \end{cases}$$

where

$$\hat{s} = \begin{cases} d_l, & \text{for basic message} \\ d_m, & \text{for additional message.} \end{cases}$$

Then, the interference at the receiver from an interferer i, I_i, when the interferer i transmits a packet, is

$$I_i = P_i d_i^{-n}$$

where P_i is the adjusted transmission power of the interferer i, d_i is the distance between the interferer i and the receiver. Then, the total interference, I, at the receiver is

$$I = \sum_{i \in T} I_i,$$

where T is the set of interferers which transmit simultaneously with the packet under consideration.

Let Z be signal to interference and noise ratio $(SINR)$ at the receiver. Then,

$$Z = \begin{cases} \frac{S_{r,S}}{N_o + I}, & \text{if } M = 1 \\ \frac{S_{r,U}}{N_o + I}, & \text{if } M = 0. \end{cases}$$

where M is the indicator that indicates a radio simulcasting when $M = 1$, or unicasting when $M = 0$. Now, the transmitted packet is considered as collided at the receiver when $Z < \gamma$, where γ is the target $SINR$. We measure the throughput efficiency defined as throughput per unit energy consumption,

$$\begin{aligned} S_{lf} &= \frac{S}{\overline{P}} \\ S_{ef} &= \frac{S_{ete}}{\overline{P}}, \end{aligned}$$

where S_{lf} and S_{ef} are the link throughput efficiency and end-to-end throughput efficiency, respectively. S, S_{ete}, and $\bar{P}$ are link throughput, end-to-end throughput, and average power consumption.

6.3 Simulation Results

We let the target error probability be 10^{-4}, the transmission range by unicasting without power control, R, be $1Km$, the original transmission power, P_o, for the target error probability at the boundary R be 1, and the thermal noise, N_o, be -8.4dB. The simulation was carried out over G from 0 to 1. The optimal G to maximize the link and the end-to-end throughput is variable, and the effect of power control on the link and the end-to-end throughput is quite different over the range of G. So, we measure the performances of the link and the end-to-end throughput as the summation of the link and the end-to-end throughput over G from 0.1 to 1, which includes the *maximal attempt rate*, G_m, which maximize the throughputs and call them the "*total link throughput*" and "*total end-to-end throughput*", respectively.

Figure 6–5 shows the simulation results for link throughput in (a), link throughput efficiency in (b), end-to-end throughput in (c), and end-to-end throughput efficiency in (d). The results indicate that link throughput as well as throughput efficiency can be increased by properly allocating transmission power. For the link and the end-to-end throughputs, the performances increase as both α and β increase, and at the α values over 3, they are almost saturated. For the link and the end-to-end throughput efficiencies, the performances are not so sensitive to α as to β, but have a greater dependence on β. By allocating the transmission power unequally with power allocation weights of $\beta = 1.0$ and $\alpha = 2.5$, the link and the end-to-end throughput efficiencies increase about 34.4% and 34.3%, respectively, with degradation of 17.8% and 15% for the link and the end-to-end throughput, respectively. Depending on the applications, the weights can be chosen to provide a trade off between throughput and throughput efficiency. For example, by allocating $\beta = 1.6$ and $\alpha = 2.5$, the link and the end-to-end throughput efficiencies increase about 15.6% and 16.0%, respectively, with degradation of only 6.7% and 4.0% for the link and the end-to-end throughput, respectively, compared to the maximum values we found.

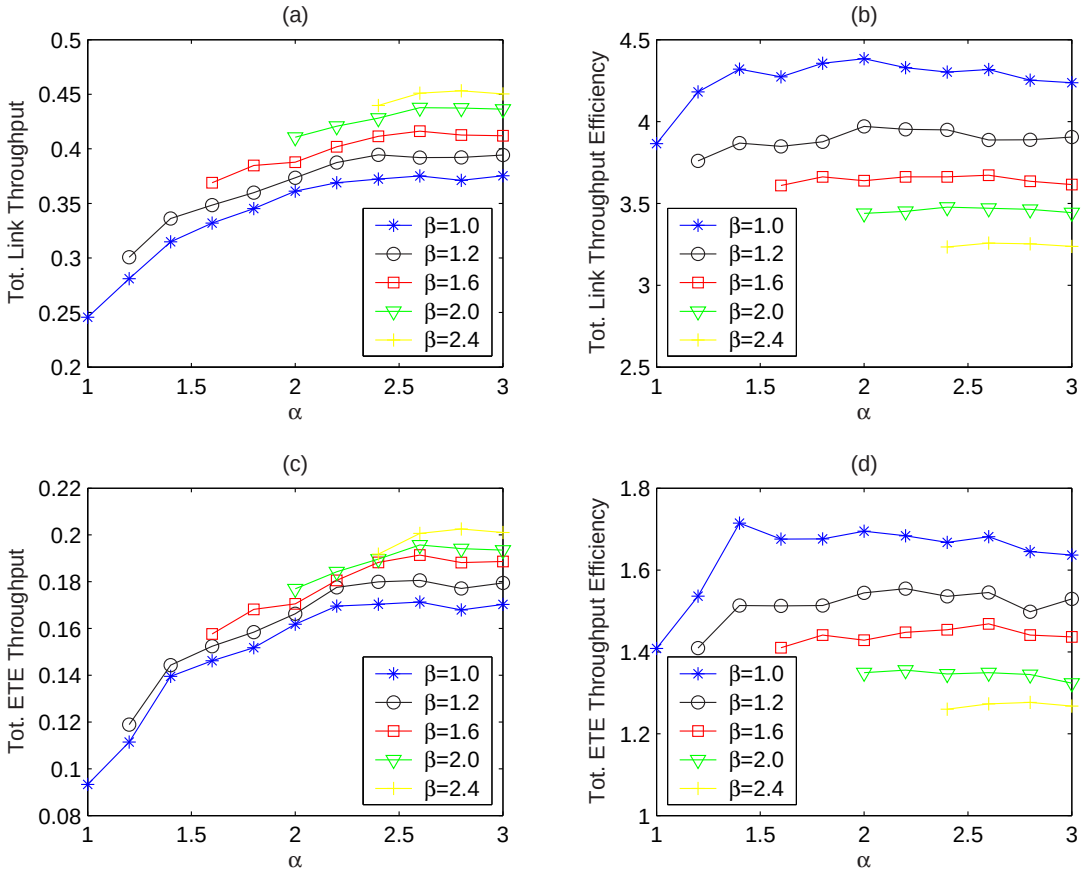

Figure 6–5. Throughput and throughput efficiency by unequal transmission power allocation.

Figure 6–6 shows the simulation results of MMI in (a), UFI with $\alpha^F = 0.0$ in (b), UFI with $\alpha^F = 0.5$ in (c), and UFI with $\alpha^F = 1.0$ in (d) as discussed in Chapter 4. Fairness in terms of MMI decreases from 0.22 to 0.05 as β decrease from 2.4 to 1.0 over the range of α greater than 2. In terms of UFI, it decreases from 0.75 to 0.60 at the same variation of α and β. All the fairness index which include the MMI and the UFIs with three different α^F has similar patterns. That means the unequal transmission power allocation doesn't significantly affect the tradeoff between *service fairness* and *effort fairness*.

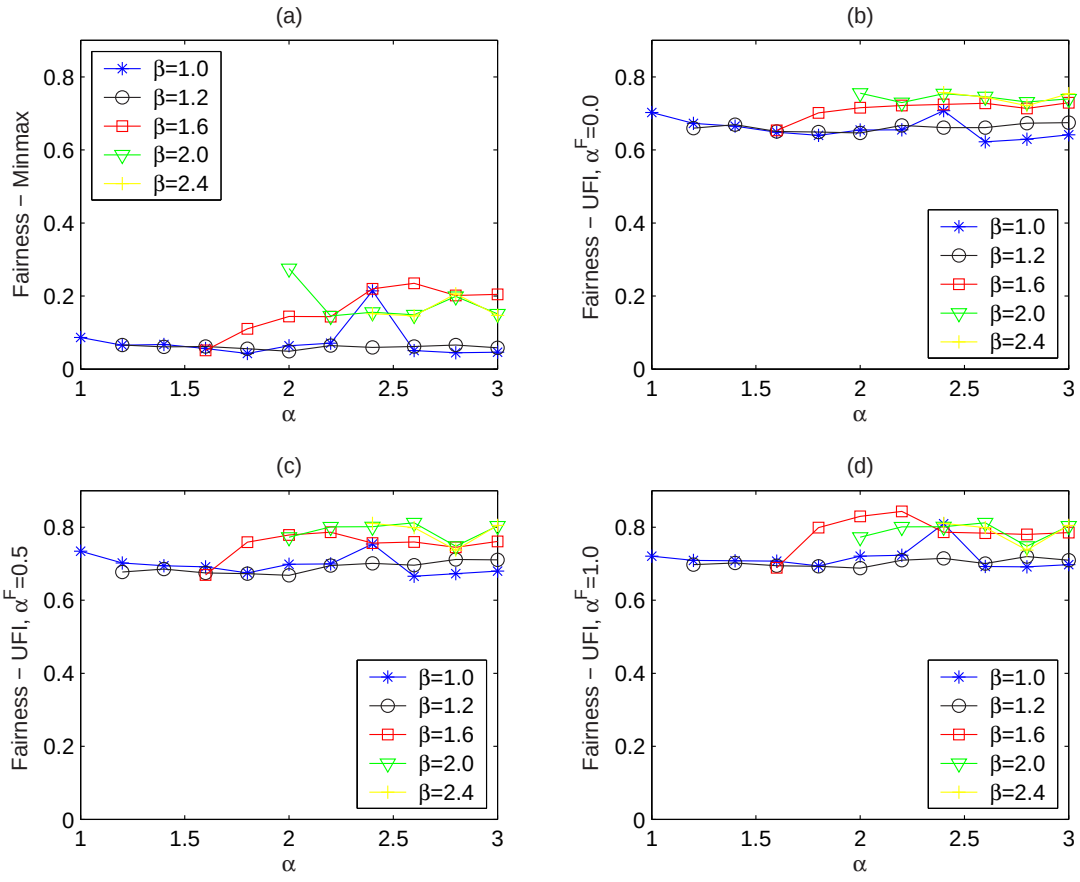

Figure 6–6. Fairness by unequal transmission power allocation.

CHAPTER 7
CONCLUSIONS

We introduced the use of simulcast transmission techniques for ad hoc networks. We applied a cross-layer approach in which the link- and network-layer protocols were modified to effectively utilize the new capability presented by simulcasting. We proposed some modifications to the routing, packet-selection, and back-off algorithms. The performance of simulcast signaling was analyzed and simulated for a network that employs slotted ALOHA. We presented detailed results on the effects of varying the offset angle θ when nonuniform QPSK is used for simulcasting. We showed that we cannot simply increase the signal constellation size to a larger constellation with uniform spacing without severely affecting the network connectivity and end-to-end throughput. The analytical and simulation results confirm that by choosing the simulcasting parameters appropriately, simulcasting can significantly improve both link and end-to-end throughput for static networks at the expense of a slight decrease in network connectivity.

Unequal resource allocations were studied to effectively utilize simulcasting capability. First, modifications to the back-off parameters were simulated. A priority-based MAC protocol was investigated in which the retransmission probabilities were increased for those radios that have a more-capable receiver and decreased for those radios that have only less-capable links. Increasing the priority was found to allow a higher average link throughput to be achieved at high average attempt rates. Second, we investigated random multiple route selection based on the simulcasting capabilities of the radios along two routes in a system that employs multi-path routing. The simulation results show that the end-to-end throughput was substantially increased by using multiple routes and assigning greater transmission rates along the more-capable route. Third, unequal transmission power for simulcasting was investigated. The simulation results

show that throughput and throughput efficiency defined as throughput per unit power consumption are increased by assigning relatively higher transmission power to the radio simulcasting. Overall, unequal resource allocation for simulcasting increases throughput and throughput efficiency at a certain expense of fairness.

REFERENCES

[1] T. M. Cover, "Broadcast channels," *IEEE Trans. Inform. Theory*, vol. IT-18, pp. 2-14, Jan. 1972.

[2] P. P. Bergmans and T. M. Cover, "Cooperative broadcasting," *IEEE Trans. Inform. Theory*, vol. IT-20, pp. 317-324, May 1974.

[3] M. B. Pursley and J. M. Shea, "Phase-shift-key modulation for multimedia multicast transmission in mobile wireless networks," in *Proc. 1996 IEEE Military Commun. Conf.*, vol. 1, (McLean, VA), pp. 210-214, Oct. 1996.

[4] M. B. Pursley and J. M. Shea, "Nonuniform phase-shift-key modulation for multimedia multicast transmission in mobile wireless networks," *IEEE J. Select. Areas Commun.*, vol. 5, pp. 774-783, May 1999.

[5] M. B. Pursley and J. M. Shea, "Multimedia multicast wireless communications with phase-shift-key modulation and convolutional coding," *IEEE J. Select. Areas Commun.*, vol. 17, pp. 1999-2010, Nov. 1999.

[6] M. B. Pursley and J. M. Shea, "Adaptive nonuniform phase-shift-key modulation for multimedia traffic in wireless networks," *IEEE J. Select. Areas Commun.*, vol. 18, pp. 1394-1407, Aug. 2000.

[7] L. G. Roberts, "Aloha packet system with and without slots and capture," *Computer Commun. Review*, vol. 5, pp. 28-42, Apr. 1975. Originally distributed as ARPA Satellite System Note 8 on June 26, 1972.

[8] I. Gitman, "On the capacity of slotted ALOHA networks and some design problems," *IEEE Trans. Commun.*, vol. COM-23, pp. 305-317, Mar. 1975.

[9] N. Abramson, "The throughput of packet broadcasting channels," *IEEE Trans. Commun.*, vol. 25, pp. 117-128, Jan. 1977.

[10] D. Bertsekas and R. Gallager, *Data Networks*. Prentice-Hall, 1991.

[11] W. Stallings, *Data and Computer Communications*. Prentice Hall, 7th ed., 2003.

[12] A. Goel, A. Meyerson, and S. Plotkin, "Combining fairness with throughput: Online routing with multiple objectives", in *Proc. 32nd ACM Symp. on Theory of Computing*, 2000, pp. 670-679.

[13] Mehrdad Dianati, et al., "A New Fairness Index for Radio Resource Allocation in Wireless Networks", *IEEE commun. society*, pp. 712-717, 2005.

[14] Mohammad Mahfuzul Islam, “Min-max Fairness Scheme for Resource Allocation in Cellular Multimedia Networks”, in *Proc. Int. Conf. Inform. Technol.: Coding and Computing(ITCC ’05)* - Vol. II, 2005, pp. 271-276.

[15] M.-S. Alouini, X. Tang, and A. Goldsmith, “An adaptive modulation scheme for simultaneous voice and data transmission over fading channels,” in *Proc. 1998 Vehic. Technol. Conf.*, vol. 2, (Ottawa, Canada), pp. 939-942, May 1998.

[16] M.-S. Alouini, X. Tang, and A. Goldsmith, “An adaptive modulation scheme for simultaneous voice and data transmission over fading channels,” *IEEE J. Select Areas Commun.*, vol. 17, pp. 837-850, May 1999.

[17] P. Vitthaladevuni and M.-S. Alouini, “BER computation of 4/M-QAM hierarchical constellations,” *IEEE Trans. Broadcasting*, vol. 47, pp. 228-239, Sept. 2001.

[18] P. Vitthaladevuni and M.-S. Alouini, “A recursive algorithm for the exact BER computation of generalized hierarchical QAM constella-tions,” *IEEE Trans. Inform. Theory*, vol. 49, pp. 297-307, Jan. 2003.

[19] B. Masnick and J. Wolf, “On linear unequal error protection codes,” *IEEE Trans. Inform. Theory*, vol. IT-3, pp. 600-607, Oct. 1967.

[20] A. R. Calderbank and N. Seshadri, “Multilevel codes for unequal error protection,” *Trans. Inform. Theory*, vol. IT-39, pp. 1234-1248, July 1993.

[21] P. Hoeher, “Unequal error protection for digital mobile DS- CDMA radio systems,” in Proc. 1994 IEEE Int. Conf. on Commun., vol. 3, (New Orleans, Louisiana), pp. 1236-1241, May 1994.

[22] G. Caire and G. Lechner, “Turbo codes with unequal error protection,” *Electronics Letters*, vol. 32, pp. 629-631, Mar. 1996.

[23] G. Caire and E. Biglieri, “Parallel concatenated codes with unequal error protection,” *IEEE Trans. Commun.*, vol. 46, pp. 565-567, May 1998.

[24] A. Heubner, J. Freudenberger, R. Jordan, and M. Bossert, “Irregular turbo codes and unequal error protection,” in *Proc. 2001 IEEE Int. Symp. Inform. Theory*, (Washington, D.C.), p. 142, June 2001.

[25] L.-F. Wei, “Coded modulation with unequal error protection,” *IEEE Trans. Commun.*, vol. COM-41, pp. 1439-1449, Oct. 1993.

[26] M. Sajadieh, F. R. Kschischang, and A. Leon-Garcia, “Modulation-assisted unequal error protection over the fading channel,” *IEEE Trans. Vehic. Technol.*, vol. 47, pp. 900-908, Aug. 1998.

[27] R. H. Morelos-Zaragoza, M. P. C. Fossorier, S. Lin, and H. Imai, “Multilevel coded modulation for unequal error protection and multistage decoding-part I: Symmetric constellations,” *IEEE Trans. Commun.*, vol. 48, pp. 204-213, Feb. 2000.

[28] M. Isaka, M. P. C. Fossorier, R. H. Morelos-Zaragoza, S. Lin, and H. Imai, “Multi-level coded modulation for unequal error protection and multistage decoding-part II: Asymmetric constellations,” *IEEE Trans. Commun.*, vol. 48, pp. 774-786, May 2000.

[29] E. G. Larsson, “Unitary nonuniform space-time constellations for the broadcast channel,” *IEEE. Commun. Letters*, vol. 7, pp. 21-23, Jan. 2003.

[30] Yun Li and Anthony Ephremides, “Simple Rate Control for Fluctuating Channels in Ad Hoc Wireless Networks”, *IEEE Trans. Commun.*, vol. 53, No. 7, pp. 1200-1209, Jul. 2005.

[31] C.-K. Toh, *Wireless ATM and Ad-Hoc Networks: Protocols and Architectures*. Kluwer, 1997.

[32] A. Kumar and J. Kleinberg, “Fairness measure for resource allocation”, in *Proc. IEEE Symposium on Foundation of Computer Science*, 2000, pp. 568-578.

[33] H. Suzuki and F. A. Tobagi, “Fair bandwidth reservation scheme with multi-link and multi-path routing in ATM networks”, in *Proc. of IEEE INFOCOM*, 1992.

[34] P. Narvaez and K. Y. Siu, “Efficient Algorithm for Multi-Path Link State Routing”, *ISCOM ’99*, Kaohsiung, Tiwan, 1999.

[35] S. Vutukury and J. J. Garcia-Luna-Aceves, “A Simple Approximation to Minimum-Delay Routing”, SIGCOMM ’99, Sept. 1999.

[36] D. Thaler and C. Hopps, “Multipath Issues in Unicast ans Multicast Next-hop Selection”, *IETF RFC 2001*, 2000.

[37] L. Kleinrock and J.A. Silvester, “Optimum transmission radii for packet radio networks or why six is a magic number,” in *Proc. IEEE Nat. Telecommun. Conf.*, Dec. 1978, pp. 4.3.1-4.3.5

[38] Hideaki Takaki and L. Kleinrock, “Optimal transmission ranges for randomly distributed packet radio terminals,” *IEEE Trans. Commun.*, vol. COM-32, pp-246-257, Mar. 1984.

[39] T.C. Hou and V.O. K. Li, “Transmission range control in multihop packet radio networks,” ion in mobile wireless networks,” *IEEE Trans. Commun.*, vol. COM-34, pp-38-44. Jan. 1986.

[40] E. S. Sousa and J. A. Sivester, “Optimum transmission ranges in a direct sequence spread spectrum multihop packet radio network,” *IEEE J. Select. Areas Commun.*, vol. 8, No. 5, pp. 762-771, June 1990.

[41] E. M. Royer, P. M. Melliar-Smith, and L. E. Moser, “An analysis of the optimum node density for Ad hoc mobile networks,” in *Proc. IEEE ICC 2001*, vol. 3, pp. 857-861

[42] P. Gupta and P.R. Kumar, “Critical power for asymptotic connectivity in wireless networks,” in *Stochastic Analysis, Control, Optimization and Applications: A volume in Honor of W.H. Fleming*(W. M. McEneany, G. Yin, and Q. Zhang, eds.), pp. 547-566, Boston, MA: Birkhauser, Mar. 1998. ISBN 0-8176-4078-9.

[43] P. Gupta and P.R. Kumar, “The capacity of wireless networks,” *IEEE Trans. Inform. Theory*, vol. IT-46, pp. 338-404, Mar. 2000.

[44] N. Bambos and G. Pottie, “Power control based admission policies in cellular radio networks,” in *GLOBECOM ’92*.

[45] G. J. Foschini, “A simple distributed autonomous power control algorithm and its convergence,” *IEEE Trans. Vehic. Technol.*, vol. 42, pp. 641-646, Nov. 1993.

[46] A. Goldsmith, “Capacity and dynamic resource allocation in broadcast fading channels,” in *Proc. 33rd Annual Allerton Conf. Commun., Control and Computing*, pp. 915-924.

[47] S. Grandhi, J. Zander, and R. Yates, “Constranined power control,” *Int. J. Wireless Personal Commun.*, vol. 1, no. 4, 1995.

[48] D. Mitta, “Asynchronous distributed algorithm for power control in cellular radio systems,” in *Proc. 4th WINLAB Workshop*, Oct. 1993, pp. 249-257.

[49] P. Viswanath, V. Anantharam, and D. Tse, “Optimal sequences, power control and capacity of synchronous CDMA systems with linear MMSE multiuser receivers,” *IEEE Trans. Inform. Theory*, vol. 45, pp. 1968-1983, Sept. 1999.

[50] J. Zander, “Transmitter power control for co-channel interference management in cellular radio systems,” in *Proc. 4th WINLAB Workshop*, 1993.

[51] N. Bambos, “Toward power-sensitive network architectures in wireless communications,” *IEEE Personal Commun., vol. 5*, pp. 50-59, June 1998.

[52] S. Hanly and D. Tse, “Power control and capacity of spread-spectrum wireless networks,” *Automato.*, vol. 35, no. 12, pp. 1987-2012, 1999.

[53] N. Bambos and S. Kandukuri, “Power control multiple access (PCMA),” *Wireless Networks*, 1999.

[54] A. Chockalingam and M. Zorzi, “Energy efficiency of media access protocos for mobile data networks,” *IEEE Trans. Commun.*, vol. 46, pp. 1418-1421, Nov. 1998.

[55] M. Abranmowiz and I. A. Stegun, “*Handbook of Mathematical Functions with Formulas, Graphs, and Mathematical Tables*”, Dover Pub., p. 68.

[56] William Navidi and Tracy Camp, “Stationary Distributions for the Random Waypoint Mobility Model”, *IEEE Trans. on Mobile Computing*, vol. 3, No. 1, Jan.-Mar. 2004

[57] Christian Bettstetter et al., “The Node Distribution of the Random Waypoint Mobility Model for Wireless Ad Hoc Networks”, *IEEE Trans. Mobile Computing*, vol. 2, No. 3, Jul.-Sep. 2003.

[58] Jungkeun Yoon *et al.*, “Random Waypoint Considered Harmful”, 2003.

[59] Jean-Yves Le Boudec, “Understand the Simulation of Mobility Models with Palm Calculus”, *Technical Report IC*, Jul. 2004.

[60] M. B. Pursley, H. B. Russell, and J. S. Wysocarski, EUROCOMM 2000. information Systems for Enhanced Public Safety and Security. IEEE/AFCEA, pp. 1-5, 17 May 2000.

BIOGRAPHICAL SKETCH

Kiung Jung received the B.S. and M.S. degrees in Electronic Material Engineering from Kwangwoon University, Seoul, Korea in 1988 and 1990, respectively, and the M.S. degree in Electrical and Computer Engineering from University of Florida, Gainesville, FL, in 2001. From 1990 to 2002, he was with Electronics and Telecommunications Research Institute (ETRI), Taejon, Korea, where he was mainly involved in the project of developing TDX-10 digital switching system, and CDMA Mobile Communication System. His current research is on wireless communication with emphasizing physical layer signaling, application of error control coding, ad hoc network, collaborative communications, cross-layer (physical – MAC) design in ad-hoc network.